

**Investigate the Effects of Piperazine Designer Drugs on Amyloid Beta**  
by

AISHAH ALI HARSHAN

A thesis submitted to the Graduate Faculty of  
Auburn University  
in partial fulfillment of the  
requirements for the Degree of  
Master of Science

Auburn, Alabama  
August 8, 2020

Keywords: Beta Amyloid, Designer Drugs, 3-TFMPP, 3-TFMBzPP, Alzheimer's disease,  
Piperazines

Copyright 2020 by AISHAH ALI HARSHAN

Approved by

Tim Moore, Professor, Research Programs and Drug Discovery and Development  
Murali Dhanasekaran, Professor, Drug Discovery and Development  
Jack DeRuiter, Ph.D. Professor, Drug Discovery and Development  
C. Randall Clark, Ph.D. Professor, Drug Discovery and Development

## Abstract

Designer drugs are structurally novel compounds that can exhibit several pharmacodynamic effects. The diverse pharmacodynamic effects of designer drugs are due to their significant interaction with the major drug targets in the body. The designer drugs can interact with several receptors, enzymes, and reuptake pumps which can lead to pharmacological or toxicological effects. Currently, there is a great prophylactic and therapeutic need to decrease the risk of neurodegeneration. Alzheimer's disease is a neurodegenerative disorder that induces irreversible cognitive impairment. Based on the current therapeutic demand to decrease the risk associated with Alzheimer's disease, there is an immediate need to develop new drugs with neuroprotective effects. Amyloid-beta ( $A\beta$ ) and tau pathologies are mainly attributed to the neurodegeneration in Alzheimer's disease. Therefore, in this study, we elucidated the effect of piperazine designer drugs on amyloid-beta ( $A\beta$ ) metabolism. We used PS70 cells to evaluate the neuroprotective effects of piperazine designer drugs against  $A\beta$  neurotoxicity. Initially, we evaluated the effects of piperazine designer drugs (3-TFMPP-parent compound and 3-TFBzPP-derivative) on PS70 cell viability. Regarding the mechanism of cytotoxicity, we assessed the effects of piperazine designer drugs (3-TFMPP and 3-TFBzPP) on the markers of oxidative stress, mitochondrial function, apoptosis, and inflammation. The parent compound, 3-TFMPP, exhibited higher toxic effects due to the increased generation of pro-oxidants & decreased antioxidants, enhanced apoptosis and inflammatory markers as compared to the piperazine derivative, 3-TFMBzPP. We used non-toxic doses of 3-TFMPP and 3-TFMBzPP to study the effect on  $A\beta$  metabolism. 3-TFMBzPP exhibited significant neuroprotective effect as compared to 3-TFMPP. The neuroprotective effects of 3-TFMBzPP is attributed to their effect on amyloid precursor protein, and gamma ( $\gamma$ )-secretase which resulted in decreased  $A\beta$ -42 formation. Furthermore, we

also validated our findings using molecular modelling. Thus, 3-TFMBzPP may be a potent molecule that can be used to reduce A $\beta$ -induced neurodegeneration. Our further studies will use valid animal model to validate the *in vivo* neuroprotective effects against A $\beta$  and tau pathologies.

## **Acknowledgements**

First and foremost, I would like to thank Almighty Allah for giving me the energy, courage, endurance and determination to accomplish this work.

I would like to express my sincere gratitude to My advisors and committee members Dr. Timothy Moore. Dr. Muralikrishnan Dhanasekaran, Dr. Randall Clark and Jack Deruiter, for allowing me to undertake this work and for their patience and guidance in assisting me overcome the difficulties I have faced during the experiments and research.

Also, I am sincerely grateful my parents for their continuous support, love, encouragement, and they are always behind all the success I have achieved in my life. At last but not least, I thank my sponsor, the Saudi Ministry of Health, for granting me the scholarship to pursue my graduate studies.

## Table of contents

<i>Abstract</i> .....	<i>II</i>
<i>Acknowledgements</i> .....	<i>IV</i>
<i>Table of contents</i> .....	<i>V</i>
<i>Table of Contents</i> .....	<i>V</i>
<i>List of Figures</i> .....	<i>IX</i>
<i>List of tables</i> .....	<i>XI</i>
<i>List of Abbreviations</i> .....	<i>XII</i>
<i>Introduction</i> .....	<i>1</i>
<i>Chapter 1: Literature review</i> .....	<i>3</i>
<b>1. Alzheimer’s disease (AD)</b> .....	<b>3</b>
<b>2. Amyloid Beta (A<math>\beta</math>)</b> .....	<b>5</b>
<b>2.1 Formation of Amyloid Beta Peptide</b> .....	<b>5</b>
<b>2.2 Classification of Amyloid Beta</b> .....	<b>7</b>
<b>2.3 Degradation of Amyloid Beta</b> .....	<b>7</b>
<b>2.4 Physiological role of Amyloid beta</b> .....	<b>10</b>
<b>2.4 A<math>\beta</math> induce neurotoxicity</b> .....	<b>13</b>
<b>2.5 A<math>\beta</math> neurotoxicity prone to cellular defects</b> .....	<b>14</b>
<b>3. Alzheimer’s disease and inflammation</b> .....	<b>16</b>

<b>4. Treatment of AD.....</b>	<b>17</b>
<b>a. Nonpharmacologic therapy:.....</b>	<b>17</b>
<b>b. Pharmacological treatment of cognitive symptoms:.....</b>	<b>17</b>
<b>c. Pharmacological treatment of non-cognitive symptoms.....</b>	<b>18</b>
<b>5. Designer drugs .....</b>	<b>19</b>
<b>a. Piperazines designer drugs chemical structure .....</b>	<b>19</b>
<b>b. Pharmacology of Piperazine drugs .....</b>	<b>20</b>
<b>c. Piperazine Toxicity and Treatment .....</b>	<b>21</b>
<b>6. Effects of stimulants on Amyloid Beta.....</b>	<b>22</b>
<b>a. CNS Stimulants.....</b>	<b>22</b>
<b>b. Effect of Caffeine on Amyloid Beta .....</b>	<b>22</b>
<b>c. Effect of Methamphetamine on Amyloid Beta .....</b>	<b>24</b>
<b><i>Chapter two: Materials and Methods .....</i></b>	<b><i>24</i></b>
<b>I. Chemical and reagents: .....</b>	<b>25</b>
<b>II. Methods .....</b>	<b>25</b>
<b>1.Cell culture .....</b>	<b>25</b>
<b>2.Treatment strategies: .....</b>	<b>26</b>
<b>3.Cell viability assay .....</b>	<b>27</b>
<b>4.Protein quantification: .....</b>	<b>27</b>
<b>5.Western blot analysis: .....</b>	<b>27</b>
<b>6.<math>\alpha</math>-secretase activity assay: .....</b>	<b>28</b>
<b>7.Y- secretase activity assay: .....</b>	<b>28</b>

8.A $\beta$ ELISA assay:.....	28
9.Neprilysin activity assay: .....	28
12.Molecular docking .....	28
13.MM/GBSA.....	29
14.Determination of ROS generation: .....	29
15.Estimation of lipid peroxidation: .....	30
16.Nitrite assay: .....	30
17.Mitochondrial Complex-I activity: .....	31
18.Glutathione content .....	31
19.Hydrogen Peroxide content: .....	31
20.NADH content: .....	31
22.Caspase-1 activity:.....	32
23.Caspase-3 activity: .....	32
24.Caspase-8 activity:.....	32
28.Caspase-9 activity:.....	32
29.COX activity: .....	32
30.Neprilysin activity: .....	<b>Error! Bookmark not defined.</b>
31.Protease activity: .....	33
<b>III. Statistical analysis:.....</b>	<b>34</b>
<b><i>Chapter three: Results</i>.....</b>	<b>35</b>
<b>I. Effects of 3-TFMPP (parent compound) and 3-TFMBzPP derivatives on PS70 cell viability .....</b>	<b>35</b>
<b>II.Pharmacodynamic effects of 3TFMPP and 3TFMBzPP .....</b>	<b>41</b>

<b>III.Effect of TFMPP parent piperazine its structural derivative (3-TFMPP and 3-TFMBzPP) on Amyloid-beta (A<math>\beta</math>) metabolism in PS70 cells .....</b>	<b>44</b>
<b>IV.Effect of piperazine designer drug and its derivative (3-TFMPP and 3-TFMBzPP) on various pro-oxidant markers in the PS70 cells: .....</b>	<b>53</b>
<b>V.Effect of piperazine designer drug and its derivative (3-TFMPP and 3-TFMBzPP) on various antioxidant markers in the PS70 ovarian cells: .....</b>	<b>58</b>
<b>VI.Effect of piperazine designer drug and its derivative (3-TFMPP and 3-TFMBzPP) on mitochondrial function in the PS70 cells:.....</b>	<b>60</b>
<b>VII.Effect of piperazine designer drug and its derivative (3-TFMPP and 3-TFMBzPP) on inflammatory markers in the PS70 ovarian cells: .....</b>	<b>62</b>
<b>VIII.Effect of piperazine designer drug and its derivative (3-TFMPP and 3-TFMBzPP) on apoptosis markers in the PS70 cells: .....</b>	<b>64</b>
<b><i>Discussion</i> .....</b>	<b>70</b>
<b><i>References:</i>.....</b>	<b>74</b>



## List of Figures

Figure 1: The nonamyloidogenic and amyloidogenic pathways of APP processing. ....	6
Figure 2: chemical structures of Piperazine compounds (Arbo et al.,2012). ....	20
Figure 3. Effect of Hydrogen peroxide on PS70 cells.....	36
Figure 4: 3-TFMPP induced significant dose and time dependent on PS70 ovarian cell toxicity: 38	
Figure 5: 3-TFMBzPP induced significant dose and time dependent on PS70 cell toxicity: .....	40
Figure 6: Effect of 3-TFMPP and 3-TFMBzPP on gamma secretase .....	45
Figure 7: Effect of 3-TFMPP and 3-TFMBzPP on alpha secretase .....	46
Figure 8: Effect of 3-TFMPP and 3-TFMBzPP neprilysin activity .....	47
Figure 9: . Effect of 3-TFMPP and 3-TFMBzPP on (A $\beta$ )-42 content.....	48
Figure 10: Effect of 3-TFMPP and 3-TFMBzPP on (A $\beta$ )-42 expression .....	49
Figure 11: Effect of 3-TFMPP and 3-TFMBzPP on APP $\alpha$ expression.....	50
Figure 12: Effect of 3-TFMPP and 3-TFMBzPP on beta secretase expression .....	51
Figure 13: Effect of 3-TFMPP and 3-TFMBzPP on total APP expression.....	52
Figure 14: Effect of 3-TFMPP and 3-TFMBzPP on ROS generation.....	55
Figure 15: Effect of 3-TFMPP and 3-TFMBzPP on nitrite content .....	56
Figure 16: Effect of 3-TFMPP and 3-TFMBzPP on lipid peroxide content .....	57
Figure 17: Effect of 3-TFMPP and 3-TFMBzPP on glutathione content .....	59
Figure 18: Effect of 3-TFMPP and 3-TFMBzPP on Complex-1 activity .....	61
Figure 19: Effect of 3-TFMPP and 3-TFMBzPP on cyclooxygenase activity.....	63
Figure 20: Effect of 3-TFMPP and 3-TFMBzPP on caspase 3 activity .....	66
Figure 21: 3-TFMPP and 3-TFMBzPP on caspase8 activity .....	67

Figure 22: 3-TFMPP and 3-TFMBzPP on caspase 9 activity .....	68
Figure 23: 3-TFMPP and 3-TFMBzPP on protease activity .....	69

## List of tables

Table 1. Stages of Alzheimer’s disease and their corresponding symptoms.....	4
Table 2: AD medications and their adverse effects.....	18
Table 3&Table 4: Pharmacodynamic effects of 3TFMPP and 3TFMBzPP .....	41
Table 5: Computational analysis for Alpha secretase .....	42
Table 6: Computational analysis for beta secretase.....	42
Table 7: Computational analysis for gamma secretase .....	43
Table 8: Effect of 3-TFMPP and 3-TFMBzPP on Hydrogen peroxide content.....	58
Table 9: Effect of 3-TFMPP and 3-TFMBzPP on NADH content .....	61
Table 10: Effect of 3-TFMPP and 3-TFMBzPP on Caspase 1 activity .....	63

## List of Abbreviations

APP- Amyloid precursor protein

A $\beta$  -Amyloid beta

AICD -APP intracellular domain

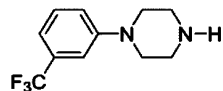
FAD -Familial Alzheimer's disease

SAD- Sporadic Alzheimer's disease

IDE -The insulin-degrading enzyme

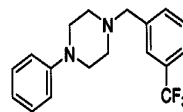
TFMPP-Trifluoromethylphenyl piperazine

TFMBzPP- Trifluoro-Methyl-Benzyl-Phenylpiperazine



3-TFMPP

## Introduction



3-TFMBzPP

Designer drugs are illegally synthesized to produce the psychostimulatory effects similar to the banned psychotic drugs of abuse. Piperazine designer drugs were initially formulated due to the legal banning of amphetamine (Scheduled Substance of Abuse). Apart from their psychostimulatory effects, designer drugs induce mental, movement, and memory-related adverse effects. However, the designer drugs have shown to exhibit several pharmacodynamic effects. Based on their pharmacodynamic effects, it has the ability to modulate the functions in the body. Thus, designer drugs in a non-toxic dose can be used pharmacologically to treat various disorders.

The current global peril is the distressing rise in the number of Alzheimer's disease patients. The extracellular senile plaques that accumulate in the brain of Alzheimer's patients are caused by amyloid-beta ( $A\beta$ ) through sequential cleavages of amyloid- $\beta$  precursor protein (APP) by  $\beta$  and  $\gamma$ -secretase. Interestingly, drugs that modulate  $A\beta$  pathway are considered to be one of the most promising avenues for treating Alzheimer's disease. However, the role of piperazine on the pathophysiology of  $A\beta$  metabolism is not well elucidated. The purpose of this study is to investigate the effects of piperazine derivatives on  $A\beta$  metabolism. PS70 cells-Chinese Hamster Ovarian (CHO) cells (carrying the amyloid precursor protein-APP and Presenilin PS1 mutation) are valid *in vitro* model for this study. Piperazine derivatives dose-dependently inhibited the PS70 cell proliferation. Furthermore, based on our drug-based computational analysis, we will elucidate the interaction of Piperazine derivatives with various markers of ( $A\beta$ ) metabolism. Thus, our

current study will help to shed more light on the effects of Piperazine derivatives on the A $\beta$  pathology in Alzheimer's disease.

## **Chapter 1: Literature review**

### **1. Alzheimer's disease (AD)**

Alzheimer's disease is the most prevalent form of dementia (Prince, M., et al, 2016). Alzheimer's disease is a neurodegenerative disorder that is mainly characterized by neuropsychiatric issues, loss of physical function, cognitive decline, and cholinergic neuronal loss in the hippocampus and cortex (Wells, B et al., 2014). In the United States, Alzheimer's disease is considered the sixth leading cause of death in the country. As of the year 2020, almost 5.6 million Americans aged 65 and older suffer from Alzheimer's disease (Prince et al., 2016). By 2050, 13.8 million Americans are estimated to be living with Alzheimer's disease (Hebert, L et al., 2013). Currently, Alzheimer's disease's financial burden surpasses \$230 billion and is expected to hit \$1.1 trillion by 2050 (Alzheimer's Association, 2012). The rise in Alzheimer's condition raises the concern of understanding the related component and what triggers its spread. Pathologically, Alzheimer's disease is characterized by abnormal accumulation of extracellular A $\beta$  plaques and intracellular neurofibrillary tangles composed of hyperphosphorylated tau protein (Bayer, T. A., & Wirths, O., 2010 and Kumar, A., & Singh, A. 2015). Therefore, it is necessary to understand A $\beta$  peptide as a component that is found in plaques and hyperphosphorylated tau protein as a component found in neurofibrillary tangles, and both are accountable for the occurrence of Alzheimer's disease. A $\beta$  peptide is produced from the sequential cleavage of the transmembrane cell surface protein amyloid precursor protein (APP). A $\beta$  is produced when APP is first cleaved by  $\beta$ -secretase and then by  $\gamma$ -secretase (Chow et al., 2010). A $\beta$  peptide accumulate in the brain of Alzheimer's patients by aggregating first into oligomers and then into larger fibrils. There is no cure for Alzheimer's disease, partly due to the fact that the pathogenesis of this disease is still not well understood. Therefore, understanding the role of A $\beta$  plaques contributing to the occurrence

of neurodegeneration at the molecular level will enhance our understanding of Alzheimer's disease and may contribute to an effective treatment for Alzheimer's disease.

Alzheimer's disease was first discovered in 1906 by Alois Alzheimer in one of his patients, Auguste Detor. The patient had been exhibiting abnormal behavior and cognitive impairment since her admission to the Frankfurt hospital where Dr. Alzheimer worked in 1901. Dr. Alzheimer followed Detor's case for five years. After her death, Dr. Alzheimer performed an autopsy, and found senile plaques and neurofibrillary tangles (Hippius, H., & Neundörfer, G. 2003). Based on the time of disease onset, Alzheimer's disease is classified into two types: Familial Alzheimer's disease (FAD) and sporadic Alzheimer's disease (SAD) (Bekris et al., 2010). Alzheimer's disease is mainly caused by genetic mutations (70%) and environmental factors (30%). Mutations in APP, PSEN1, or PSN2 genes are responsible for inducing FAD, while in sporadic Alzheimer's disease, the genetic mutation occurs in the APOE gene (Dorszewska et al.,2016). Early-onset Alzheimer's disease occurs in individuals under age 65 and represents almost 1% to 6% of all cases, while late-onset Alzheimer's disease affects people above age 65 (Bekris et al., 2010). Several risk factors attribute to Alzheimer's disease including aging, genetics, head injury, depression, decreased brain capacity due to decreased physical activity or decreased level of education, and vascular diseases (Edwards lii et al., 2019). Depending on the severity of the symptoms, Alzheimer's disease is known to enter three stages: mild, moderate, and severe (Table 1) (Wells, et al., 2014).

Table 1. Stages of Alzheimer's disease and their corresponding symptoms.

<b>Stage</b>	<b>Symptoms</b>
Mild	Difficulty to remember the recent events, struggle to manage finance or prepare food and get lost while driving
Moderate	Difficulty remembering the recent events, forget specific details of past life, disoriented with regard to time, agitation, delusions, and paranoia. Usually, the patient requires assistance with daily life activities.
Severe	Lose the ability to walk, speak, and feed, Incontinent of urine and feces. Usually, patient Requires care 24 hours a day.



## 2. Amyloid Beta (A $\beta$ )

### 2.1 Formation of Amyloid Beta Peptide

A $\beta$  Peptide is cleaved from APP, a type 1 integral membrane glycoprotein expressed in various tissues, particularly in neuronal synapses. Neuronal synapses play a crucial role in the pathogenesis of Alzheimer's disease, as alterations in synapse structure and function and defective synaptic transmission are believed to cause neurodegeneration (Chen et al., 2017). APP is found as several isoforms, of which the three main isoforms are APP751, APP770, and APP695. The APP695 isoform is the most abundant in the brain and it is distinguished from the other isoforms as it is lacking the Kunitz-type serine protease inhibitory sequence (KPI) (Guerreiro, Gustafson & Hardy, 2012). KPI is involved in various physiological functions, such as blood clotting, blocking of ion channels, inflammation, and fibrinolysis (Wan et al., 2013). After APP is synthesized in the endoplasmic reticulum (ER), it is transported to the Golgi complex, where it completes maturation. Then, it is eventually transported to the plasma membrane (Jiang et al., 2014). The mature APP is initially sliced by either  $\alpha$ -secretase (nonamyloidogenic pathway) or  $\beta$ -secretase (amyloidogenic pathway) to produce membrane-tethered  $\alpha$ - or  $\beta$ -C terminal fragments (CTFs). sAPP $\alpha$  is released from the cell surface when APP is cleaved by  $\alpha$ -secretase, leaving an 83-amino-acid C-terminal APP fragment. In response to neuronal activity and activation of muscarinic acetylcholine receptors, the production of sAPP $\alpha$  increases, proposing that neuronal activity raises the  $\alpha$ -secretase cleavage of APP (Mattson, 2004). The Carboxyterminal fragment that is produced from  $\alpha$ - and  $\beta$ - secretase cleavage of APP undergoes intramembrane cleavage by  $\gamma$ -secretase to produce P3 and A $\beta$  peptides, respectively (Chow et al., 2010). In the amyloidogenic pathway, APP is cleaved sequentially by  $\beta$ -secretase, which is also known as the trans-membranous aspartic

protease  $\beta$ -site APP cleaving enzyme 1 (BACE1), at the N-terminal region of the extracellular domain of APP. This leaves the membrane-anchored fragment and following  $\gamma$ -secretase cleavage at the intramembranous region,  $A\beta$  is released. Specifically, APP is cleaved by  $\beta$ -secretase to produce a 99-amino-acid C-terminal fragment of APP (C99) that is subjected to further cleavage by  $\gamma$ -secretase to generate the hydrophobic  $A\beta$  fragment and liberate the APP intracellular domain (AICD) (Zheng & Koo, 2011). AICD then transfers to the nucleus, where gene expression can be regulated, including apoptotic genes such as CASP6, GSK3, and p53, and as such AICD may play a role in the pathogenesis of Alzheimer's disease by inducing neuronal death (Ozaki et al., 2006).

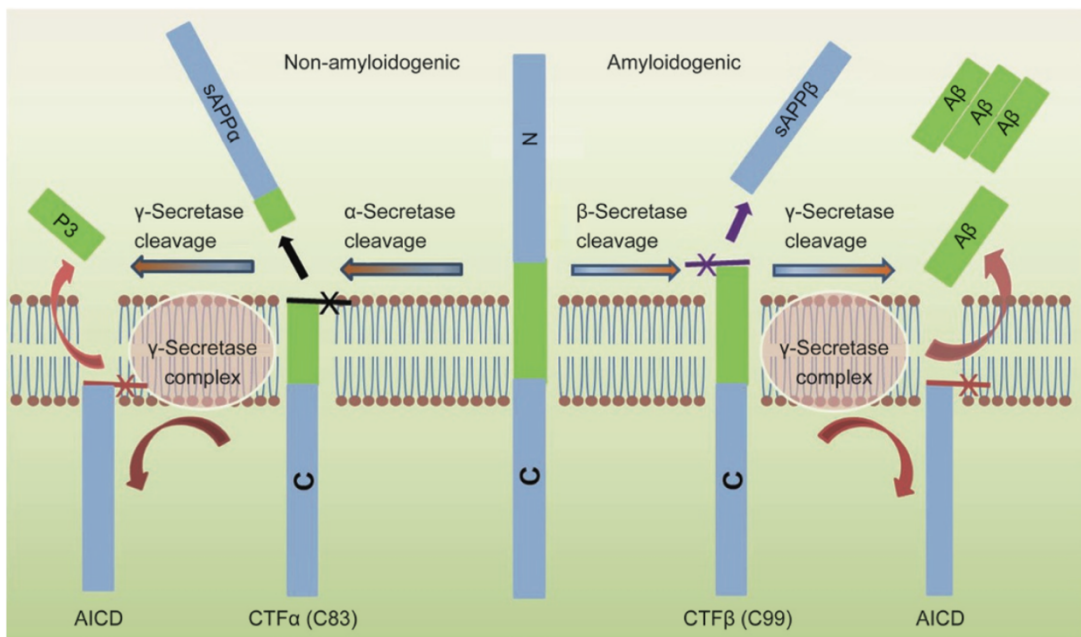


Figure 1: The nonamyloidogenic and amyloidogenic pathways of APP processing.

APP is cleaved by alpha- or beta-secretase. Cleavage by alpha-secretase (the nonamyloidogenic pathway) produces sAPP-alpha and C83. Cleavage by beta-secretase (the amyloidogenic pathway) produces sAPP-beta and C99. C83 is cleaved by gamma-secretase, generating AICD and p3. C99 is also cleaved by gamma-secretase, generating AICD and  $A\beta$  (Chen, G et al., 2017)

## **2.2 Classification of Amyloid Beta**

According to the structure, A $\beta$  peptides are classified into A $\beta$  monomer, A $\beta$  oligomer, A $\beta$  protofibril, and A $\beta$  fibril. A $\beta$  monomers are aggregated into different assembly forms, such as oligomers, protofibrils, and amyloid fibrils. A $\beta$  monomers possess neuroprotective activity. This neuroprotective activity is believed to be mediated by the phosphatidylinositol-3-kinase (PI-3-K) pathway, which involves the (insulin-like growth factor-1) IGF-1 receptor or other members of the insulin receptor superfamily. In contrast, A $\beta$  oligomers have neurotoxic effects (Giuffrida et al.,2010). In neurons suffering from trophic factors deprivation wherein there is a lack of support from trophic factors such as nerve growth factor (NGF), the synthetic monomeric A $\beta$  has a rescue effect mediated by activation of the pathway of phosphatidyl- inositol-3-kinase (PI-3-K), which is an essential neuronal survival pathway (Giuffrida et al.,2009). Meanwhile, amyloid fibrils are larger and insoluble and assemble to form A $\beta$  plaques in the brain of Alzheimer's patient (Ow& Dunstan, 2014).

## **2.3 Degradation of Amyloid Beta**

In a healthy adult, the A $\beta$  production process should be accompanied by another balancing factor that maintains the amyloid level in equilibrium and prevents the deleterious consequences. Therefore, A $\beta$  production is generally counterbalanced by multiple processes, such as proteolytic degradation, cell-mediated clearance, active brain transport, and deposition into insoluble aggregates (Saido& Leissring, 2012).

### **a. Proteolytic degradation of Amyloid Beta**

Proteolytic degradation is a vital determinant of A $\beta$  in the brain and becomes an extension of the disease associated with A $\beta$  (Saido & Leissring, 2012). Many enzymes play a vital role in the degradation cycle of the A $\beta$ . These enzymes include individual amyloid beta-degrading neprilysin proteases, insulin-degrading enzymes, endothelin-converting enzymes, and plasmin, among other amyloid beta-degrading proteases (Baranello et al., 2015).

Neprilysin, a type 2 membrane glycoprotein, is a zinc metallo-endopeptidase, and it has a vital role in degrading amyloid beta peptides. The optimum pH of neprilysin is neutral, so after synthesis, neprilysin is translocated to the plasma membrane (presynaptic membrane,) to display full activity. Neprilysin degradation of A $\beta$  is likely to occur at or near synapses and may also occur within secretory vesicles if APP and neprilysin are located in the same vesicles. The activity of neprilysin is decreased with aging (Iwata, Higuchi & Saido 2005). Therefore, neprilysin deficiency leads to the development of Alzheimer's disease by increasing the accumulation of A $\beta$  (Iwata et al., 2001).

The endothelin-converting enzymes are an integral membrane-bound protease class II, which belongs to the same zinc metallopeptidases family M13 as neprilysin. The ECEs convert the inactive endothelin to its potent vasoactive peptide endothelin-1 (ET-1) (Palmer et al., 2009). Also, the ECE-1 and ECE-2 act as proteolytic degradation of A $\beta$  (Chen et al., 2017 and Eckman, Reed & Eckman, 2001). The two ECE isoforms, ECE-1 and ECE-2, have a sequence homology of 59 percent and identical catalytic activity; however, the optimal pH of ECE-1 is neutral, the optimum pH of ECE-2 is 5.5 (Emoto & Yanagisawa, 1995). ECE-2 and ECE-1 are localized intracellularly, whereas other sub isoforms of ECE-1 are restricted in the plasma membrane (Schweizer et al., 1997 and Pacheco & Eckman 2013).

The insulin-degrading enzyme (IDE) is a 110-kDa zinc metallopeptidase located in the cytosol, peroxisomes, cell surfaces, and endosomes (Farris et al.,2003). According to genetic studies, the IDE region of chromosome 10q is related to DM2, as well as the late onset of Alzheimer's disease (Bertram,2000). IDE degrades A $\beta$ , and it has an indirect impact on A $\beta$  level through its influence on AICD, which is involved in transcriptional regulation of APP (Puthuchery et al.,2011). Therefore, IDE eliminates the extracellular A $\beta$  and AICD, a cytoplasmic product of gamma- secretase cleaves APP.

Besides neprilysin, ECE, and IDE, there are many enzymes that contribute to degrading A $\beta$ , such as angiotensin converting enzyme (ACE), plasmin, and matrix metalloproteases. ACE regulates blood pressure by cleaving Angiotensin I to Angiotensin II and then inactivating bradykinin (Puthuchery et al.,2011). According to genetic studies, there is a relationship between Alzheimer's disease and ACE: insertion of polymorphism in the ACE gene is associated with protective effect because insertion polymorphism increases ACE level that assists to degrade A $\beta$  (Hemming & Selkoe 2005).

Finally, plasmin is a serine protease produced by the cleavage of plasminogen by tissue plasminogen activator (tPA). Normally, plasmin plays a role in fibrinolytics, but it is also an example of an A $\beta$ -degrading protease (Jacobsen, 2008).

#### **b. Cell-mediated clearance**

Several mechanisms of A $\beta$  degradation are mediated by glial cells that produce proteases, such as neprilysin, IDE, and ECE, as well as glial cells release extracellular chaperones, such as apolipoproteins,  $\alpha$ 1-antichymotrypsin and  $\alpha$ 2macroglobulin that are involved in clearance of A $\beta$  (Ries & Sastre,2016)

### **c. Autophagy**

A $\beta$  can be eliminated by astrocytes, microglia, and macrophages via phagocytosis, followed by degradation by Cathepsin B that is located in endosomes and lysosomes, or by ECE enzymes (Ries & Sastre,2016). Moreover, many studies show that A $\beta$  is degraded by the autophagy-lysosome pathway. There was a study that demonstrated that estrogen receptor beta (ER $\beta$ ) enhances the degradation of A $\beta$  and exhibits neuroprotective effects by activation of autophagy (Wei et al., 2019). The microtubule associated protein 1 light chain 3 (LC3) is an important protein in autophagy as it is needed for the formation of autophagosomes and their membranes. After formation, LC3 is cleaved by Atg4 to form LC3I, and LC3I is then converted to LC3II. As such, LC3II levels are proportional to the formation of autophagosomes, and hence LC3II is used as a marker for autophagy. Therefore, A $\beta$  neurotoxicity is reduced by overexpression of LC3II, which is done by promoting alpha nicotinic acetylcholine receptor ( $\alpha$ 7nAChR) (Hung et al.,2015). ATG7 or autophagy related 7 is an essential protein for the formation autophagosomes during autophagy, particularly during the initiation of autophagy, and it also plays a role in the conversion of LC3I to LC3II. Various studies showed that performing knockdown of the ATG7 gene decreases the expression of  $\alpha$ 7nAChR (Hung et al.,2009& Wei et al.,2019).

### **2.4 Physiological role of Amyloid beta**

Despite the predominant notion that A $\beta$  causes neurotoxic or deleterious effects leading to Alzheimer's disease, caution must be taken in developing treatment/management options that deal with A $\beta$  as soluble A $\beta$  has been shown to play various physiological roles even in normal individuals. Soluble A $\beta$  are distributed throughout the brain and body and performs several physiological functions involving synaptic-function and modulation, fostering neuronal growth

and survival, protection from oxidative stresses, and surveillance of pathogens, toxins, and neuroactive compounds (Bishop& Robinson, 2014). The involvement of A $\beta$  in synaptic function and modulation is believed to occur as A $\beta$  exerts a trophic function at low concentrations. This then has implications on both memory and learning. Similarly, physiological levels of A $\beta$  is also necessary for neuronal survival, again due to its proposed neurotrophic effects at low concentrations (Yan, S. D., & Stern, D. M. 2005). Thus, development of treatment modalities for Alzheimer's disease which target A $\beta$  should be done while taking into account these functions of soluble A $\beta$ , and perhaps the target of such therapies may be shifted to forms of A $\beta$  which permit aggregation or accumulation (Bishop& Robinson, 2014).

**a. Modulation of synaptic function**

One of the more prominent clinical features of Alzheimer's disease is memory impairment. To elucidate the pathophysiology behind this clinical feature, a vast number of studies have been done to figure out the role of A $\beta$  or APP contributing to memory impairment. At normal physiological concentrations, A $\beta$  is essential for synaptic activity (Pearson& Peers2006). There was a study done on APP transgenic mice and wild type mice. The transgenic mice had fewer synapses compared to the control. Additionally, the transgenic mice showed impaired long-term potentiation (LTP) (Dawson et al. & Seabrook et al., 1999) that can be rescued by injection of A $\beta$  (Puzzo et al.,2011). The APP transgenic mice also performed poorly on spatial memory tasks (Dawson et al. & Seabrook et al., 1999). A $\beta$  enhances LTP in picomolar concentrations, and in turn this activates alpha 7-nicotinic acetylcholine receptor, increasing the release of acetylcholine into the synaptic cleft; however, at higher (nanomolar) concentrations of A $\beta$ , the alpha 7-nicotinic acetylcholine receptor was blocked (Paris et al.,2010). Inducing hippocampal neuronal activity in brain slices promotes the production of A $\beta$  and AICD that modulates synaptic activity (Kamenetz

et al.,2003). At the physiological level, APP serves as a negative feedback that depresses synaptic activity to prevent the excitotoxicity produced from excessive activity of synapse (Puzzo et al.,2011). The duration of exposure is essential to determine the effects of A $\beta$  on synaptic plasticity. A $\beta$  enhances the synaptic plasticity within minutes; however, with prolonged exposure, the synaptic plasticity is reduced (Koppensteiner et al., 2016). Therefore, high doses of A $\beta$  impair memory while lower doses enhance memory.

#### **b. Promoting neuronal growth and survival**

Several studies have shown that A $\beta$  plays a vital role in neuronal development and survival. Membrane phospholipids concentration and expression of APP, Tau, and GAP-43-growth associated proteins are increased in primary neuronal culture by adding nanomolar concentration of the A $\beta$  (1-40) isoform, indicating that A $\beta$  (1-40) may promote neurite formation (Wang et al.,2000). Moreover, the neuronal viability is decreased by 20-50 % compared to the control when  $\gamma$ - or  $\beta$ - secretase, essential to cleave APP to form A $\beta$ , are inhibited. Interestingly, the decrease in neuronal viability can be restored by adding 10pmol/L to 1nmol/L of A $\beta$  (Plant et al.).

#### **c. Protection Against Oxidative Stress**

Some studies prove that A $\beta$  acts as a prooxidant while other studies confirm that A $\beta$  acts as an antioxidant (Mitra et al, 2019). Usually, A $\beta$  is released by neurons and can be found in cerebrospinal fluid (CSF) and plasma. Kontush et al. (2001) proved that using (0.1-1.0nM) of A $\beta$  inhibited CSF autooxidation. However, using a high concentration of A $\beta$  (10-100nM) abolished the antioxidant action of A $\beta$  (Kontush et al.,2001). As such, the concentration of A $\beta$  regulates oxidative stress, it acts as an antioxidant in low concentrations and prooxidant in high concentrations.



#### **d. Antimicrobial activity**

A $\beta$  is an antimicrobial peptide (AMP) that is considered as a class of innate immune defense. It protects the host from a variety of pathogens by forming fibrils that entrap the infectious agents and disrupt the cell membranes (Gosztyla et al., 2018). A study was done to confirm the antimicrobial activity of A $\beta$ . The proliferation of seven species of bacteria and one fungus was decreased by adding 25 $\mu$ g/mL of A $\beta$ 42 (Gosztyla et al., 2018). However, this concentration (25  $\mu$ g/mL) exceeds the physiological level of A $\beta$ , and consequently, this antimicrobial activity is not effective in representing the *in vivo* experiment. To overcome this limitation, the homogenates of temporal cortex of Alzheimer's patient could be used, as they are more effective in inhibiting *Candida albicans* than the homogenate of a normal person (Soscia et al.,2010). Moreover, the antimicrobial activity of A $\beta$  was confirmed by using mice and nematodes model of Alzheimer's disease that enhance resistance to bacterial infections such as *Salmonella typhimurium meningitis* in this animal (mice) model of Alzheimer's disease (Kumar et al.,2016).

### **2.4 A $\beta$ induce neurotoxicity**

A $\beta$  peptide is produced and released into the extracellular space and generates a toxic signal into neurons through the plasma membrane. A $\beta$  is capable of binding directly to cell membranes, as well as ion channels or spores that induce damage of the membrane which may cause neuronal damage (Kam, Gwon & Jung, 2014). Moreover, A $\beta$  oligomers that are neither fibrils nor monomers but are soluble increase the permeability of the membrane, hence dysregulating Ca<sup>2+</sup> signals for neurotoxicity (Demuro et al., 2005). A $\beta$  binds to receptors like N-methyl-D-aspartate (NMDA) to produce neuronal toxicity, especially the oligomers A $\beta$  that induces dysfunction in mitochondria and oxidative stress, causing a massive increase in Ca<sup>2+</sup> influx and neuronal toxicity (Canevari et al.,2004).

### **a. NMDA receptor and A $\beta$**

N-methyl-D-aspartate receptor (NMDA) is one of the ionotropic glutamate receptors and has subunits NR1, NR2 (A, B, C, and D), and NR3 (A and B) (Cull-Candy et al.,2001). A $\beta$  oligomers bind to the NMDA receptor, particularly to NR1/NR2A and NR1/NR2B subunits. This binding induces direct activation of NMDA, which dramatically increases the intracellular level of Ca<sup>2+</sup>. Neuronal death that can be prevented by using memantine, an NMDA antagonist (exidó et al. .2011).

### **b. $\alpha$ 7nAChR receptor and A $\beta$**

$\alpha$ 7 nicotinic acetylcholine receptor is an ion channel receptor that's essential for cognitive function (Kadir et al., 2006). A $\beta$  oligomers have a high affinity to bind to  $\alpha$ 7nAChR and activate it, leading to phosphorylation of tau protein via ERK and JNK pathway (Oz et al.,2013).

### **c. p75 neurotrophin receptor (P75NRT) and A $\beta$**

p75 neurotrophin receptor also called low-affinity nerve growth receptor, has structure similar to TNFR1- tumor necrosis factor receptor 1, CD40, and Fas. A $\beta$  binds to P75 receptor at its death domain (Ser337–Ser416), inducing cell death via apoptosis by activation caspase-8 and caspase-3, also, through production ROS (Fisone et al., 2004).

## **2.5A $\beta$ neurotoxicity prone to cellular defects**

### **a. A $\beta$ toxicity induces Endoplasmic Reticulum Stress (ER) stress**

ER senses and response to numerous changes in cellular conditions to maintain the folding capacity of the protein through the unfolded protein response (UPR) (Ron & Walter 2007). Unfolded protein response is a recovery system in cells in response to ER stress to reduce the overload on the ER. Accumulation of misfolding or unfolding protein in the lumen of the ER leads to the activation of UPR. Three major pathways of UPR that are controlled by protein kinase (R-

like ER kinase (PERK), inositol requiring kinase 1 (IRE1) as well as stimulating transcription factor 6-ATF6). Prolonged PERK activation elicits the death of cells by expressing C/EBP-homologous protein that hinders anti-apoptotic B cell lymphoma 2 (Bcl-2) transcription (McCullough et al.,2001). Salubrinal, which is a discriminatory protein phosphatase1 inhibitor, counters PERK by dephosphorylating eIF2 $\alpha$ . It is defensive alongside the neurotoxicity of A $\beta$  (Huang et al., 2012). The ER in Alzheimer's disease is hampered by numerous pathologic circumstances, for instance, Ca<sup>2+</sup> dysregulation (Kam, T et al., 2014). Since the functionality of ER chaperones is altered by ER Ca<sup>2+</sup> level, the interrupted ER Ca<sup>2+</sup> causes ER stress (Michalak et al.,2002).

#### **b. A $\beta$ toxicity induces mitochondrial dysfunction**

Normally, mitochondria generate cellular energy in the form of adenosine triphosphate (ATP) through the Krebs Cycle (citric acid cycle). However, mitochondria defects are observed in neurons of Alzheimer's disease patients (Kam et al.,2014). APP accumulates in mitochondria leading to distraction of electron transport chain and mitochondrial dysfunction (Chen et al.,2017) and ultimately decrease the production of ATP due to reduced activity of alpha - ketoglutaraldehyde dehydrogenase and pyruvate dehydrogenase in Krebs cycle, as well as expression of respiratory chain components (Lustbader et al., 2004). Moreover, A $\beta$  impairs mitochondrial axonal transport, which is essential for sustained release of neurotransmitters in presynaptic terminal (Kam et al.,2014). Also, accumulation of A $\beta$  in mitochondria contributes to interaction between A $\beta$  and proapoptotic factor alcohol dehydrogenase and cyclophilin D, leading to neurodegeneration via apoptosis (Yan et al., 2005). Therefore, interaction between mitochondrial proteins like cyclophilin D, A $\beta$ -binding alcohol dehydrogenase (ABAD), and A $\beta$  were found to arbitrate neuronal and mitochondrial stress exerted by A $\beta$  (Lustbader et al., 2004&

Du et al., 2008). Mitochondria deficient in CypD are resistant to A $\beta$  induced mitochondrial stress. Also, they prevent Ca<sup>+2</sup> induced mitochondrial swelling and produce ROS. Decreasing CypD enhances memory and learning function in the AD mouse model. Therefore, reduction of CypD could help in treating Alzheimer's disease (Du et al., 2008).

### **3. Alzheimer's disease and inflammation**

Several studies point to the role of neuroinflammation in the development of neuropathological changes in Alzheimer's disease. Soluble A $\beta$  stimulates activation of the proinflammatory component of primary microglia (Sondag, C et al., 2009). It also increases the secretion of proinflammatory cytokines such as nitric oxide, TNF $\alpha$ , and TNF $\beta$  (White, J et al., 2005). Several major epidemiological and clinical studies were reported at the beginning of the 1990s. They suggested that anti-inflammatory therapies used in diseases such as rheumatoid arthritis demonstrated protective qualities against developing Alzheimer's disease. Additionally, they showed as much as a 50 percent reduction in the risk of developing Alzheimer's disease in patients who are long-term users of NSAID (Kinney, J et al., 2018). Consequently, these studies support the hypothesis that neuroinflammation plays a critical role in the progression of Alzheimer's disease. Microglia are immune cells resident inside the central nervous system (CNS) (Sarma, J. D. 2014) and inactive in a healthy brain (Glenn et al., 1989). Accumulation of A $\beta$  leads to activation of microglia causing phagocytosis of A $\beta$  (Belmont, T et al., 2008). Nonetheless, sustained activation of the immune response has been shown to contribute to an exacerbation of Alzheimer's disease pathology, possibly due to continued activation of microglia in a feed forward loop, called reactive microgliosis (Hickman, S et al., 2008 and Meda, L et al., 1995). Several proinflammatory cytokines are involved in Alzheimer's disease such as TNF- $\alpha$ , IL-1 $\beta$ , IL-6, and NF $\kappa$ B. TNF- $\alpha$  is one of the essential proinflammatory cytokines in Alzheimer's disease and plays

a vital role in initiating and regulating the cytokine cascade (Akiyama, H et al., 2000). Increased levels of TNF- $\alpha$  in both the brains and plasma of Alzheimer's disease patients have been reported (Hang, R ET AL., 2017). A $\beta$  stimulates the production of TNF- $\alpha$  by activation of NF $\kappa$ B (Combs, C et al., 2001), a transcription factor that raises expression of proinflammatory factors such as complement and cyclooxygenase (COX) (Yamamoto, K et al., 1995).

#### **4. Treatment of AD**

##### **a. Nonpharmacologic therapy:**

Managing sleep disturbances, urinary incontinence, restlessness, and anxiety through behavioral and environmental intervention is essential for Alzheimer's disease patients (Wells, B., 2014).

##### **b. Pharmacological treatment of cognitive symptoms:**

Controlling the vital sign such as blood pressure, glucose, and cholesterol may contribute to decreasing the risk of Alzheimer's disease. Cholinesterase inhibitors (Donepezil, rivastigmine, and galantamine) and memantine are the current drugs used to treat Alzheimer's disease. Since memantine is an *N*-methyl-d-aspartate antagonist, it prevents the excitotoxicity by blocking glutamatergic neurotransmission. NMDA can be used as monotherapy or in combination with cholinesterase inhibitors. Memantine is not metabolized by the liver but is excreted mainly unchanged in the urine. Therefore, the dose of memantine should be adjusted in patients with renal impairment. The below table illustrates the doses of Alzheimer's disease medications and their adverse effects (Table-2) (Wells, B., 2014).

**Table 2: AD medications and their adverse effects**

<b>Drugs</b>	<b>Dose</b>	<b>Adverse effects</b>
Donepezil	5–10 mg daily in mild to moderate AD  10–23 mg daily in moderate to severe AD	Nausea Diarrhea Vomiting Urinary incontinence Dizziness
Rivastigmine	3–6 mg twice a day (oral solution, capsule) 9.5–13.3 mg/day (transdermal patch)	Salivation Sweating Bradycardia Headache Muscle weakness
Galantamine	8–12 mg twice a day (tablet, oral solution) 16–24 mg (extended-release capsule)	
Memantine	10 mg twice daily 28 mg daily (extended-release capsule)	Constipation Confusion Dizziness Headache

**c. Pharmacological treatment of non-cognitive symptoms**

Non-cognitive pharmacotherapy treats psychotic symptoms, disruptive behaviors, and depression. Antipsychotic drugs have been used for neuropsychiatric symptoms, but care must be taken to weigh the risks and benefits. Antipsychotics (Aripiprazole, Olanzapine, Quetiapine and Risperidone), antidepressants (Citalopram Escitalopram Fluoxetine Paroxetine Sertraline Mirtazapine Trazodone), and anticonvulsant (Carbamazepine and Valproic acid) are used in the treatment of noncognitive symptoms (Wells, B., 2014).

## 5. Designer drugs

Historically, drugs of abuse originated from diverted pharmaceutical or plant products. Nowadays, designer drugs, synthetically prepared by clandestine laboratories, have become the primary sources for drug abusers (Henderson,1988). Designer drugs ("research chemicals," "internet drugs," "legal highs") are novel psychoactive products that possibly may have same negative impacts on public health like well-known illegal substances. Chemically, designer drugs are classified into Phenethylamines, Synthetic Cathinone, Piperazines, Aminoindanes Benzofurans, Pipradrols/Piperidines, and Tryptamines. According to the pharmacological action, designer drugs are classified into stimulants and hallucinogens (Liechti, 2015).

### a. Piperazines designer drugs chemical structure

Unfortunately, there is a high prevalence of designer drugs misuse especially among young individuals at night clubs and parties. The most common designer drugs are MDMA (methylenedioxymethamphetamine) that is derived from Phenethylamine. Since banning of MDMA, piperazine derivatives continue to circumvent the law on the market. In this sense, piperazine drugs emerged on the market, mostly on the internet under different names such as ecstasy pills or "Frenzy," "Bliss," "Rapture," "Bid," "Herbal Ecstasy," "A2," "Legal E and "Legal X." They are usually consumed as tablets, capsules, or pills but also in the form of powders or liquids (Gee et al.,2005). In the USA, EU and New Zealand, piperazine drugs like BZP and mCPP are currently under control. In addition to BZP and mCPP, TFMPP is also under legal control in Brazil. The World Anti-Doping Agency (WADA) prohibits the use of piperazine drugs in competitive sports. Chemically, Piperazine moiety is a cyclic molecule with two opposing nitrogen atoms within six membered ring. Piperazine drugs can be classified into two classes, the

phenylpiperazines such as mCPP (1-(3-chlorophenyl)piperazine), TFMPP (1-(3-trifluoromethylphenyl) piperazine) and MeOPP (1-(4-methoxyphenyl) piperazine), and the benzylpiperazines such as BZP (N-benzylpiperazine) and MDBP (1-(3,4-methylenedioxybenzyl)piperazine) (figure1) (Arbo et al.,2012).

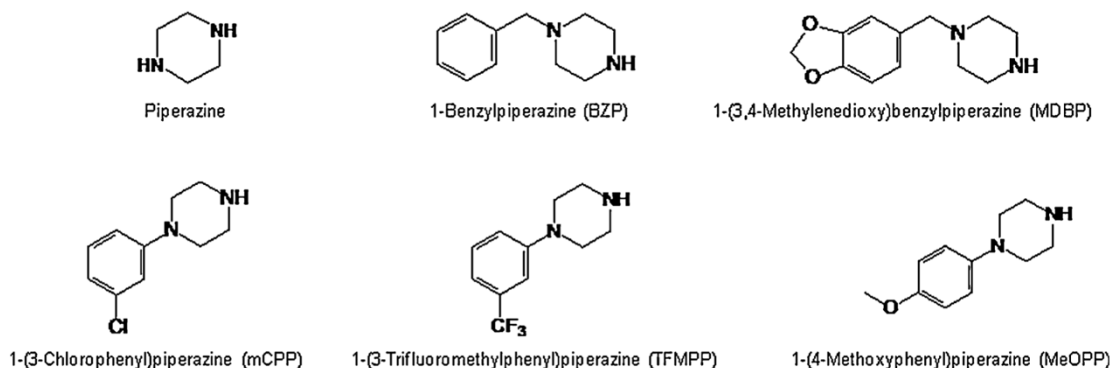


Figure 2: chemical structures of Piperazine compounds (Arbo et al.,2012).

### b. Pharmacology of Piperazine drugs

Originally, piperazine drugs were used during the 1950s as anthelmintic agents. In animals, they are still being applied in this way, but human use was gradually phased out. However, in Canada, Enactyl, an oral piperazine drug, is still available (Haroz, R and Greenberg, M, 2006). BZP is active metabolite of N-benzyl-piperazine-picolinyl fumarate, was investigated as an antidepressant in the 1970s (Schep, et al.,2011). However, in the animal studies, there were deleterious side effects, including hyperactivity, involuntary head movement, and decrease recreation time. This indicates that piperazine are sharing some properties with amphetamine. They also demonstrated that the impact of piperazines by former amphetamine addicts were not distinguished from those of dexamphetamine and found both favorable. Therefore, piperazine studies as antidepressants were not pursued (Wikström.,2004). In the United States in 2002, BZP



and TFMPP were classified as Schedule I drugs (Drug Enforcement Administration (DEA,2004). TFMPP and BZP act as MDMA; they increase the level of serotonin and dopamine. BZP raises dopamine levels more than serotonin, result in increased motor activity shown as sniffing, head bobbing, and increased ambulation. TFMPP enhances serotonin release by acting as a full agonist at serotonin receptors, except the 5HT<sub>2A</sub> receptor acts as a partial agonist/ antagonist. Nevertheless, in the equivalent doses, TFMPP is approximately three times less potent than MDMA. Remarkably, a combination of BZP with TFMPP generates a synergistic effect similar to MDMA. Additionally, motor activity is reduced when BZP is combined with TFMPP at low doses, making the experience more pleasing (Baumann et al.,2005).

### **c. Piperazine Toxicity and Treatment**

Usually, piperazines act as a stimulant at low dose and hallucinogens at the high dose. Permeability of piperazine through blood brain barrier (BB) leads to CNS intoxication such as headache, paranoia, anxiety, insomnia, and tremor. The piperazines compound is prone to deleterious side effects on the peripheral nervous system, including palpitation, vomiting, sinus tachycardia, diaphoresis, visual hallucinations, and vasoconstriction. High doses of piperazines drugs lead to severe toxicity such as seizure psychosis, respiratory acidosis, renal toxicity, and hyponatremia.

Urine immunoassay generally yields a negative result in the detection of piperazines compounds. Therefore, the most effective methods to detect piperazines drugs are mass spectrometry and gas chromatography (Dhanasekaran, M, 2018). Since no known antidote are available for piperazine, the management of individuals who are intoxicated with piperazine is supportive and requires adequate observation periods (Haroz, R and Greenberg, M, 2006). Several pharmacological and

non-pharmacological approaches to reduce piperazine-induced toxicity are the use of benzodiazepines for seizure, charcoal for oral ingested toxicity, IV fluids to maintain the vital sign, and electrocardiogram test as a safety precaution (Dhanasekaran, M, 2018).

## **6. Effects of stimulants on Amyloid Beta**

### **a. CNS Stimulants**

Psychomotor stimulants and hallucinogens act to stimulate central nervous system (CNS). The former induces euphoria and excitement, rises motor activity, and reduces the feeling of fatigue, while the latter produces changes in mood and thought patterns. Methylxanthines, Nicotine, Varenicline, Cocaine, Amphetamine, and Methylphenidate are Psychomotor stimulants. and tetrahydrocannabinol (from marijuana) and lysergic acid diethylamide (LSD) are hallucinogens (Whalen et al.,2018)

### **b. Effect of Caffeine on Amyloid Beta**

Caffeine is a methylxanthine that has a high concentration in coffee and is perhaps the greatest extensively consumed psychoactive compound across the globe (Fison et al.,2004). Caffeine has several effects on amyloid-beta, according to many studies. Caffeine is mainly metabolized in liver to paraxanthine and theophylline, both of which have physiological impacts as caffeine (Fredholm et al., 1999). Moderate concentration of caffeine (human equivalent of five cups of coffee a day) intake can decrease risk of Alzheimer's disease in transgenic (APPsw) mice by suppressing  $\beta$ -secretase and  $\gamma$ -secretase in the hippocampus (Maia, L & de Mendonca, A,2002). Acute administration of caffeine (single treatment, 1.5mg/0.2ml) reduced plasma A $\beta$  levels (Cao et al., 2009). Also, long term caffeine treatment reduced the soluble and insoluble hippocampal A $\beta$  level in young and aged APPsw mice (Arendash et al., 2006). A $\beta$  is formed in neurons and

then secreted into extracellular space and solubilized within the interstitial fluid. Based on an earlier study conducted on mice, it was evident the treatment of caffeine to AD transgenic mice decreases the levels of A $\beta$  in brain ISF- interstitial fluid as well as plasma in a span of few hours. Further, it can lead to continued reduction of plasma A $\beta$  through oral treatments within a period of one to eight weeks (Cao et al., 2009). As per recent research, a single caffeine treatment rapidly decreases equally A $\beta$  in the brain ISF as well as plasma levels of A $\beta$ 1–40 in a span of few hours hence an indication that there is an immediate and direct influence of caffeine on the brain A $\beta$  levels (Cao et al., 2009). Moreover, since blood platelets seem to be the chief source of circulating A $\beta$  and APP, it is likely that caffeine self-sufficiently lowers plasma A $\beta$  by suppressing the production of A $\beta$  from blood platelets. Generally, caffeine affects the production of A $\beta$  by suppressing both  $\gamma$ -secretase/PS1 expression as well as  $\beta$ -secretase (BACE1) (Cao et al., 2009). Previous researches indicate that; modest day-to-day consumption of caffeine could reduce or delay the hazard of AD (Ritchie et al.,2007) (Van et al.,2007). Caffeine has defensive mechanism against cognitive deficiency and AD that is associated with normal aging. As with plasma A $\beta$ , studies indicate that there was no correlation between concentrations of plasma caffeine and levels of brain A $\beta$  or cognitive performance. Higher levels of plasma caffeine are allied with lesser plasma A $\beta$  levels, although they are not contemplative of brain A $\beta$  levels or cognitive performance. Thus, plasma A $\beta$  levels is not a precise indicator of cognitive performances or brain A $\beta$  levels in aged AD mice (Cao et al., 2009). Nonetheless, research has established that caffeine is capable of acutely decreasing the brain A $\beta$  as well as the plasma A $\beta$  levels and reduces brain A $\beta$  deposition while also improving cognitive function subsequent to chronic administration (Cao et al., 2009).

### **c. Effect of Methamphetamine on Amyloid Beta**

Methamphetamine is an intensely addictive and effective stimulant in the CNS. As a psychostimulant prescription, methamphetamine has instigated severe public healthiness concerns across the globe. Exposure to methamphetamine is associated with neuroinflammation in various areas of the brain due to its addictive effect (Wongprayoon and Govitrapong, 2015). As the predecessor protein of the A $\beta$ , APP takes up significant functions in the development of Alzheimer's disease. As per previous studies, it is evident that methamphetamine has substantial effects as it increases the expression of APP in a dose-dependent manner with the highest reaction at the dosage of 1000  $\mu$ M. Moreover, the administration of methamphetamine markedly increases expression of pT205-tau, a neuropathological protein, beyond 100  $\mu$ M, further enhancing peak response at 300  $\mu$ M. Based on studies, treatment of methamphetamine (300  $\mu$ M) causes pT205-tau levels to increase intensely after six hours (Chen et al., 2019). Therefore, it is clear that methamphetamine exposure results in severe neurodegeneration and the exposure has the prospects of contributing to Alzheimer's disease-like pathological changes. Reduction in the phosphorylation of Glycogen synthase kinase-3 $\beta$  (GSK-3 $\beta$ ), as well as GSK-3 $\alpha$ , is responsible for the generation of hyper-phosphorylation of tau and APP, respectively (Zhao et al., 2011). Methamphetamine significantly decreases phosphorylated pS9-GSK3 $\beta$  and pS9- GSK3 $\alpha$ , which reflects enhanced GSK-3 $\beta$  and GSK-3 $\alpha$  activities, respectively. Therefore, chronic exposure to methamphetamine enhances the expression of APP and tau protein and ultimately impaired cognitive behaviors (Chen et al., 2019)

## **Chapter two: Materials and Methods**

## **I. Chemical and reagents:**

Designer Drugs were synthesized by Prof. Randall Clark and Prof. Jack Deruiter, Department of Drug Discovery and Development, Harrison School of Pharmacy, Auburn University. Penicillin / Streptomycin Solution was purchased from CORNING. Dulbecco's Modification of Eagle's Medium (DMEM), thiazolyl blue tetrazolium bromide (MTT) reagent, NADH Disodium Salt Trihydrate, Gentamicin, puromycin and DMSO (dimethyl sulfoxide) were bought from VWR. FBS (fetal bovine serum), o-phthalaldehyde and protease substrate were purchased from Sigma-Aldric. DCF- 2',7'- Dichlorofluorescein Diacetate, Trypsin, protease substrate (SCP0225), Thiobarbituric acid and Trichloroacetic acid-TCA were purchased from Sigma. Tetramethyl-p-phenylenediamine was bought from Alfa Aesar. Phosphoric acid was purchased from Fisher Scientific. Griess Reagent, Caspase3 substrate (AC-DEVD-AMC), caspase1 substrate (AC-YVAD-AM), caspase8 substrate (Ac-IETD-AMC), and caspase 9 substrate (Ac-LEHD-AMC) were purchased from Enzo life science. gamma-secretase substrate (565764) and  $\alpha$ -Secretase Substrate II (565767) were purchased from Calbiochem. Human A $\beta$  ELISA kit was purchased from thermo fisher scientific. Neprilysin kit was purchased from abcam.

## **II. Methods**

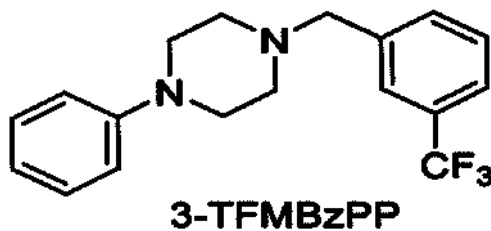
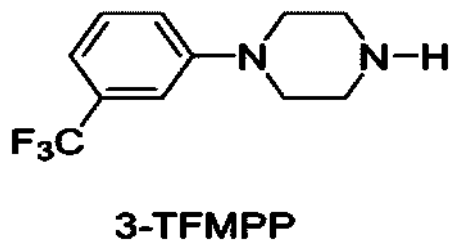
### **1.Cell culture**

To assess the effect of piperazine designer drugs and its derivatives on amyloid-beta pathology: PS70 cell lines (Chinese Hamster Ovary cells) expressing wild type human PSEN1 and Swedish mutant APP (APP<sup>swe</sup>) were used in this study. PS70 cells were cultured in 75 cm<sup>2</sup> flasks in the presence of DMEM medium, supplemented with fetal bovine serum (10%) and penicillin-streptomycin (1%) in a humidified atmosphere of 5% CO<sub>2</sub>/ 95% air at 37 °C. To preserve selection

for the expression plasmid, the cells were grown in the presence of gentamycin-G418 (200 $\mu$ g/ml) and puromycin (7.5 $\mu$ g/ml) (Ramesh et al., 2018). Depending on every experimental scale the cells were plated at an appropriate density.

## 2. Treatment strategies:

Piperazine designer drugs, parent compound and its derivatives (3-TFMPP and 3-TFMBzPP) were designed and synthesized by Dr. C. Randall Clark and Dr. Jack Deruiter. 3-TFMPP and 3-TFMBzPP were dissolved in incomplete medium to make 10mM stock solution. With respect to the cell viability assay, specific doses of piperazine derivative designer drugs (100pM, 1nM, 10nM, 100nM, 1 $\mu$ M, 10 $\mu$ M, 100 $\mu$ M, 1mM) were incubated with PS70 cells for two different time periods (24 and 48 hours). To assess the effect of piperazine designer drugs (3-TFMPP and 3-TFMBzPP) on toxicity of PS70 cells, the PS70 cells were exposed to 3-TFMPP and 3-TFMBzPP (1mM and 1 $\mu$ M) for 12 h. To assess the effects of piperazine designer drugs (3-TFMPP and 3-TFMBzPP) on amyloid beta pathology, PS70 cells were exposed to 3-TFMPP (100pM, 1nM) and 3-TFMBzPP (10nM, 1 $\mu$ M) for 48 hours. To validate the cytotoxicity of the TFMPP derivatives endogenous neurotoxins hydrogen peroxide was used as a positive control.



### **3. Cell viability assay**

The MTT assay was used to evaluate the effect of different doses of piperazine derivative designer drugs at two different time periods. The mitochondria of viable cells reduce the MTT (3-(4,5-dimethylthiazol-2-yl)-2,5-diphenyltetrazolium bromide), which is yellow color is converted to form insoluble blue crystal formazan by succinate dehydrogenases enzyme. After adding the MTT reagent to the 96 well plate, the plates were incubated for 2 hours and then the aspirate the medium, subsequently, add 200ul of DMSO was added to dissolve the crystal formazan. The resulted crystal formazan can be measured calorimetrically at 544nm. The Results are expressed as (%) change as compared to the control, Mean  $\pm$  SEM.

### **4. Protein quantification:**

Protein quantification was done by using Thermo Scientific Pierce 660nm protein assay reagent kit. BSA (bovine serum albumin) was used as standard for protein quantification.

### **5. Western blot analysis:**

Conditioned media from the control and treated cells were tested by western blot for sAPP $\alpha$ , APP, beta secretase and A $\beta$ 42. PS70 cells were lysed in RIPA buffer and equal protein amounts of cell lysates were analyzed by western blot. Before loading onto SDS-PAGE gel for protein separation, samples were denatured at 95°C for 5 minutes. Separated proteins on SDS-PAGE gel was transferred onto nitrocellulose membrane. 0.1% Tween-20 (TBST) plus 5% fat-free milk in Tris-buffered saline at pH 7.4 was used to block nonspecific binding site on nitrocellulose membranes. Then, the membranes were incubated at 4°C overnight with primary antibody that was constituted in 5% BSA in TBST. After the membranes were washed three time with TBST, the secondary antibody was added to the membranes for 1 hour at room temperature. The membranes were

washed three times with TBST after incubation with each antibody, and subsequently, the membranes were analyzed FluorChem1 system Imaging.

#### **6.α-secretase activity assay:**

Alpha secretase activity was measured fluorometrically by using specific alpha secretase substrate. The fluorescent product that formed from cleavage of substrate by alpha secretase was measured at 340/490nm.

#### **7.Gamma- secretase activity assay:**

Gamma secretase activity was measured fluorometrically by using Gamma-secretase substrate. The product that formed from cleavage of substrate by Gamma-secretase was measured at 355/440nm.

#### **8.Aβ-42 ELISA assay:**

The media was collected from treated and untreated cells to detect secreted Aβ1–42. Concentration of Aβ1–42 was measured by using ELISA kits according to the manufacture's protocol (thermo fisher scientific).

#### **9.Nepilysin activity assay:**

Nepilysin activity was assessed fluorometrically at wavelength 330/430nm by using nepilysin kits according to the manufacture's protocol (ab241003, abcam).

#### **12.Molecular docking**

Ligands were sketched in a 2D structure and converted into its 3D structure. After that, energy minimization was performed using LigPrep with OPLS3e Force field in Schrödinger software. The crystal structures of BACE1 PDB= 2ZHU, Alpha secretase PDB= 6BE6, and Gamma secretase



PDB= 6IYC were used for docking and MM/GBSA analysis. All proteins were structurally prepared by Protein Preparation Wizard utility tools in the Schrödinger Release 2019-2, Schrödinger, LLC, New York, NY. All hydrogen atoms were added to the selected proteins to optimize H-bonding interactions, missing atoms were added, and missing side chains and loops were filled. N-and C-terminal residues were specified and charged, some histidine residues were either flipped or tautomerized, while some residues were only flipped to improve H-bonding and avoid H-H clashes. Also, waters with less than 3 H-bonds to non-waters were removed. Finally, energy minimization of the protein hydrogens, water, and side chains was performed by utilizing the OPLS3e Force field. Glide docking (Schrodinger software) protocols were applied; in this docking program, the flexibility of the ligands is considered while the protein is considered as a rigid structure. The 3D coordinates of the active site were identified using grid generation. Standard precision (SP) was selected, and all other parameters were left at the default settings.

### **13.MM/GBSA**

The binding free energies ( $\Delta G_{\text{bind}}$  in kcal/mol) were calculated for each ligand from the pose view files, which were retrieved from the glide docking scores using the MMGBSA (Schrodinger software) and applied in OPLS3e Force field. The binding free energy of MMGBSA was predicted for each ligand–protein complex, as follows:  $\Delta G_{\text{bind}} = G_{\text{complex}} - G_{\text{protein}} - G_{\text{ligand}}$ , where  $\Delta G_{\text{bind}}$  is the binding free energy and  $G_{\text{complex}}$ ,  $G_{\text{protein}}$ , and  $G_{\text{ligand}}$  are the free energies of complex, protein, and ligand, respectively.

### **14.Determination of ROS generation:**

The generation of reactive oxygen species in the control and 3-TFMPP and 3-TFMBzPP treated PS70 cells was estimated spectrofluorometrically by measuring the conversion of non-fluorescent chloromethyl-DCF-DA (2', 7'- dichlorofluorescein diacetate, DCF-DA) to fluorescent DCF using

an excitation wavelength of 460nm and an emission wavelength of 528 nm . ROS generation was calculated, standardized to total protein content and reported as relative fluorescence intensity/mg protein. The fluorometric reading was estimated with BioTek Synergy HT plate reader (BioTek, VT, USA). Results were expressed as percentage change from the control. (Ahuja et al.,2017)

### **15.Estimation of lipid peroxidation:**

The lipid peroxide content was quantified using colorimetric assay procedure with thiobarbituric acid. The lipid peroxide in the control and 3-TFMPP, and 3-TFMBzPP treated PS70 cells was estimated by measuring the content of malondialdehyde (MDA) in the form of reactive thiobarbituric acid substances (TBARS). Control and designer drugs treated cell homogenate (100µl) were incubated with ice-cold 100µl Trichloroacetic acid (TCA, 20 % w/v), 400 µl Thiobarbituric acid (TBA, 0.5 % w/v) and 500µl deionized water. Following the incubation, the samples were put in a water bath at 80°C for 15 minutes and then cooling for 5 minutes then centrifuged at 10,000 RPM. The absorbance of the supernatant was measured at 532 nm in the plate reader. MDA levels were calculated as TBARS reactive substances per mg protein. (Wills et al., 1965).

### **16.Nitrite assay:**

The nitrite assay was done by using Griess reagent that contains sulfanilamide reacting with NO<sub>2</sub> under acidic condition leading to production of diazonium ion. This diazonium ion association with N-(1-naphthyl) ethylene diamine to form 36 chromophoric azo product that measured spectrophotometrically at 545nm.

### **17.Mitochondrial Complex-I activity:**

The oxidation of NADH to NAD<sup>+</sup> is catalyzed by Complex-I (NADH dehydrogenase). Cell homogenate was mixed with phosphate buffered saline and NADH to assess the activity of NADH dehydrogenase. NADH oxidation was assessed spectrophotometrically by the reduction in the absorbance at 340nm for 3 minutes (Ramsay et al.,1986).

### **18.Glutathione content:**

O-phthalaldehyde (OPT) react with Glutathione (GSH) to form fluorescence product that can be assessed spectrofluorometrically. To precipitate the protein, 120ul of cell homogenate was mixed with 12ul of the 0.1M phosphoric acid (10% of the cell homogenate) and centrifuged for 10 minutes at 2000 RPM. Then, 100ul of the supernatant was taken and incubated with 100ul OPT (0.1% w/v) and 1.8ml of PBS at room temperature for 20 minutes. The samples were read at an excitation wavelength of 340 nm and an emission wavelength of 420 nm. The GSH content was estimated as of GSH/ $\mu$ g protein (Zheng et al., 2014).

### **19.Hydrogen Peroxide content:**

Hydrogen peroxide in control and 3-TFMPP and 3-TFMBzPP treated cells content was quantified fluorimetrically.

### **20.NADH content:**

NADH in control and 3-TFMPP and 3-TFMBzPP treated cells was quantified calorimetrically at 340nm.

**22.Caspase-1 activity:**

Caspase-1 activity was measured fluorometrically by using AC-YVAD-AM substrate. The product formed from cleavage of AC-YVAD-AM substrate by caspase-1 was measured at 360/460 nm.

**23.Caspase-3 activity:**

Caspase-3 activity was measured fluorometrically by using AC-DEVD-AMC substrate. The product formed from cleavage of AC-DEVD-AMC substrate by caspase-3 was measured at 360/460 nm.

**24.Caspase-8 activity:**

Caspase-8 activity was measured fluorometrically by using Ac-IETD-AMC substrate. The product formed from cleavage of (Ac-IETD-AMC) substrate by caspase-8 was measured at 360/460 nm.

**28.Caspase-9 activity:**

Caspase-9 activity was measured fluorometrically by using Ac-LEHD-AMC substrate. The product formed from cleavage of Ac-LEHD-AMC substrate by caspase-9 was measured at 360/460 nm.

**29.COX activity:**

Cyclooxygenase activity was quantified calorimetrically by using TMPD substrate. The product formed from cleavage of TMPD substrate by cyclooxygenase was measured at 600nm (Copeland et al., 1994)

### **30. Protease activity:**

Protease activity was measured fluorometrically by using Z-Gly-Gly-Leu-7-amido-4-methylcoumarin (Z-Gly-Gly-Leu-AMC) substrate. The product formed from cleavage of substrate by trypsin-like protease was measured at 380/440nm (Usha et al., 2000).

### **32. Receptor binding assay**

Receptor binding assay for TFMPP derivatives was performed as per the protocol of National Institute of Mental Health Psychoactive Drug Screening Program (PDSP) at the University of North Carolina, Chapel Hill. Initially each isomer was tested in a primary assay at a concentration of 10uM for its ability to displace a standard ligand at each receptor and transporter subtype. Compounds which produced greater than 50% binding inhibition in the primary assay were tested further to determine receptor or transporter affinity constants ( $K_i$ : affinity of a ligand for the receptor in nM) in a secondary binding assay.

### **33. Computational Assessment**

In this study, QikProp filter from Schrödinger was used to calculate several pharmacokinetic and pharmacodynamic properties of TFMPP derivatives. Drug molecules with favorable ADME properties have been identified as the primary cause of successful candidate molecules in drug discovery and development. The QikProp set of descriptors (CNS activity, MW, HBD, HBA, QPPCaco, QPlogBB, QPPMDCK, Human Oral Absorption, % Human Oral Absorption, Rule of Five, Rule of Three) were selected to describe this aspect of the compounds permeability and activity in CNS.

## **Software**

Schrödinger Release 2019-2: QikProp, Schrödinger, LLC, New York, NY, 2019

### **III. Statistical analysis:**

Data are expressed as means  $\pm$  SEM. Statistical analyses were achieved by using one-way analysis of variance (ANOVA) followed by an appropriate post-hoc test including Tukey's and Dunnett's method ( $p < 0.05$  was considered to indicate statistical significant) statistical analyses were done using the Prism-V software (La Jolla, CA, USA)

## Chapter three: Results

### I. Effects of 3-TFMPP (parent compound) and 3-TFMBzPP derivatives on PS70 cell viability

3-TFMPP is the parent designer drug compound that has been abused globally. Interestingly, designer drug derivatives such as 3-TFMPBzPP was designed based on the modification of the chemical structure of the parent designer drug, 3-TFMPP. Hence, in the present study, we initially investigated the dose-dependent and time-dependent effects of the parent designer drug compound (3-TFMPP) on the PS70 cell viability using MTT based colorimetric method. The formazan formed due to the conversion of MTT by the active / live PS70 cells directly represents the cell viability. Thus, based on the above biochemical concept of the conversion of MTT to formazan by the cell mitochondria, we investigated the cell viability in the control (untreated ovarian cells) and designer drugs treated PS70 cells.

Parent designer drug, 3-TFMPP, dose-dependently (100pM – 1mM) decreased the PS70 cell viability. However, 3-TFMPP, only at the dose of 100uM and 1mM induced a statistically significant decrease in PS70 cell viability at 24 hours (Figure-4a,  $n = 50$ ,  $p < 0.05$ ). With regard to the percentage change, 3-TFMPP (100uM and 1mM) induced 43% and 88% dose-dependent decrease in PS70 cell viability at 24 hours. With regard to the effect of 3-TFMPP at 48 hours, dose-dependent (100pM – 1mM) decrease in the PS70 cell viability was seen which was similar to the effects observed at 24 hours. Nevertheless, a statistically significant PS70 cell toxicity of 3-TFMPP was observed from a lower dose of 10uM at 48 hours' time point. Consequently, 3-TFMPP at the dose of 10uM, 100uM and 1mM induced a statistically significant decreased PS70 cell viability at 48 hours (Figure-4,  $n = 75$ ,  $p < 0.05$ ). With regard to the percentage change, 3-

TFMPP (10uM, 100uM and 1mM) induced 41%, 63% and 93% dose-dependent decrease in PS70 ovarian cell viability at 48 hours. The endotoxin hydrogen peroxide (the positive control) induced significant dose-dependent cytotoxicity (figure -3)

Figure 3. Effect of Hydrogen peroxide on PS70 cells

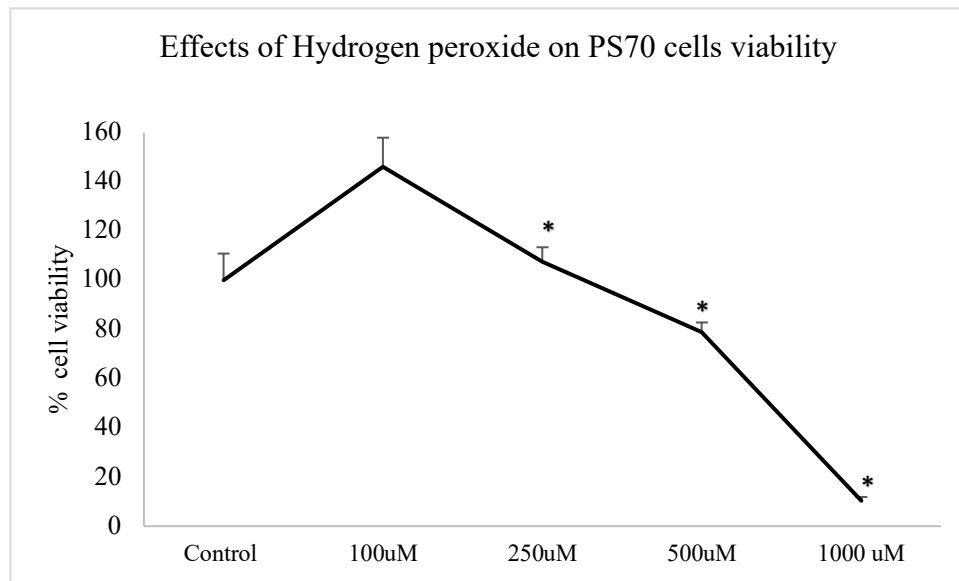
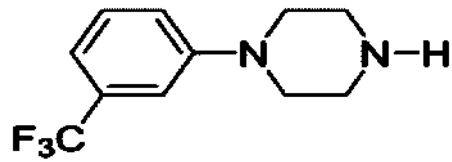


Figure-3: PS70 cells were treated with different doses of hydrogen peroxide for 24 hours. Cell viability was evaluated through the MTT reduction assay. Results are expressed as percentage control  $\pm$  SEM. Statistical comparisons were made using one-way ANOVA/ Dunnet's multiple comparison tests. Note (\*) indicates a statistically significant difference when compared to controls ( $p < 0.0001$ ,  $n=12$ )



Figure-4 a: Effect of 3-TFMPP on PS70 cells viability (24 hours)



**3-TFMPP**

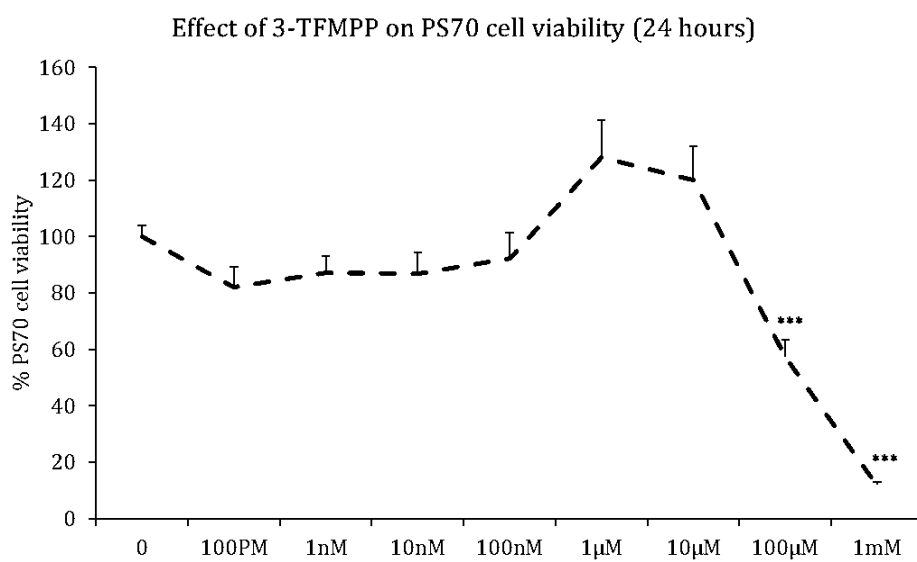


Figure-4b: Effect of 3-TFMPP on PS70 cells viability (48hours)

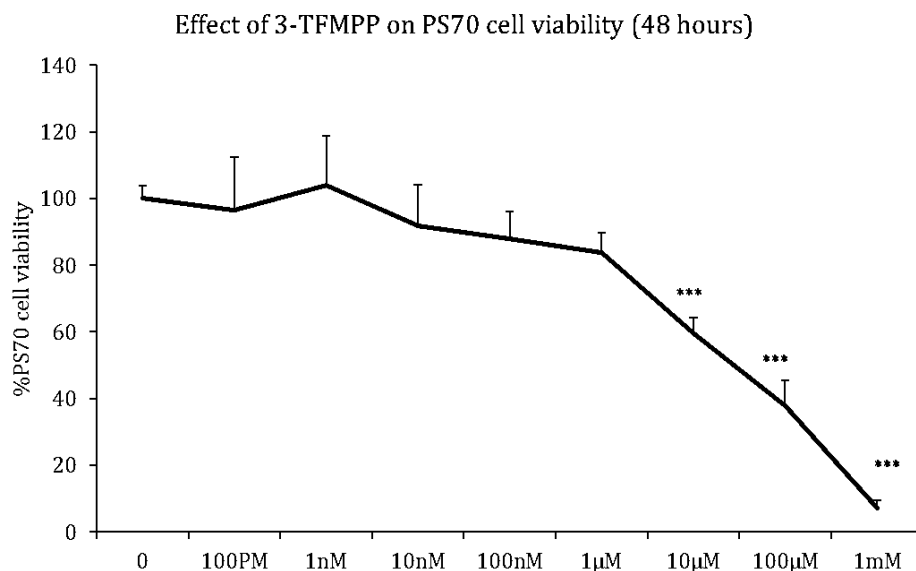


Figure 4:3-TFMPP induced significant dose and time dependent on PS70 cell toxicity:

PS70 hamster cells were treated with different concentrations of 3-TFMPP and incubated for 24 and 48 hours. MTT based colorimetric cell viability assay was used to evaluate the PS70 cells viability. Results are expressed as (%) change as compared to the control, Mean  $\pm$  SEM. 3-TFMPP dose-dependently and time-dependently decreased the PS70 cells viability significantly as compared to the control (Figure-4a and 1b,  $*p < 0.05$ ).

Effect of 3-TFMBzPP derivative on PS70 cell viability: Dose-dependent effect of 3-TFMBzPP (10pM – 1mM) on PS70 cell viability was investigated. 3-TFMBzPP, only at the high dose of 1mM induced a statistically significant decrease in PS70 cell viability at 24 hours and 48 hours (Figure-5a, b,  $n = 50, p < 0.05$ ). 3-TFMBzPP (1mM) caused 75% and 85% PS70 cell death at 24 hours and 48 hours respectively. Our results indicate that - 3-TFMBzPP induced dose-dependent and time-dependent significant PS70 cell toxicity. Moreover, as predicted the designer drug derivative, 3-TFMBzPP exhibited less toxicity as compared to the parent designer drug 3-TFMPP.

Figure-5a: Effect of 3-TFMBzPP on PS70 cells viability (24 hours)

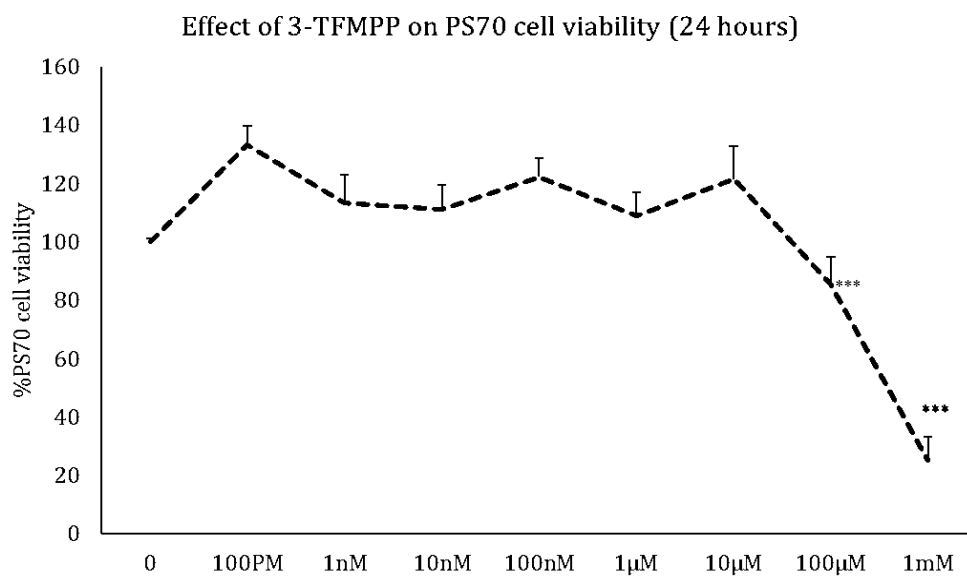
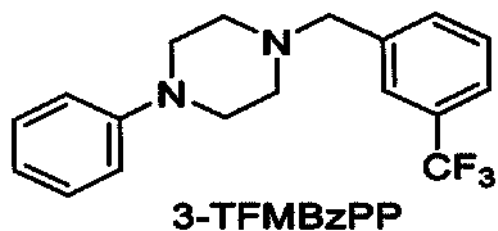


Figure 5-b: Effect of 3-TFMBzPP on PS70 cells viability (48 hours)

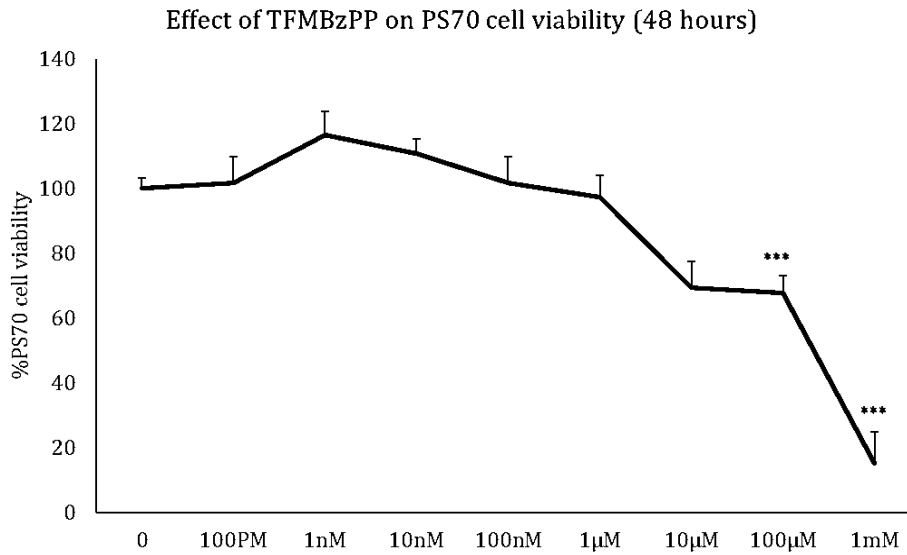


Figure 5: 3-TFMBzPP induced significant dose and time dependent on PS70 cell toxicity:

PS70 cells were treated with different concentrations of 3-TFMBzPP and incubated for 24 and 48 hours. MTT based colorimetric cell viability assay was used to evaluate the PS70 cell viability. Results are expressed as (%) change as compared to the control, Mean  $\pm$  SEM. 3-TFMBzPP dose-dependently and time-dependently decreased the PS70 cells viability significantly as compared to the control (Figure-5a and b, \* $p < 0.05$ ).

## II. Pharmacodynamic effects of 3-TFMPP and 3-TFMBzPP

Table3.

<b>Compound</b>	<b>SASA</b>	<b>FOSA</b>	<b>FISA</b>	<b>PISA</b>	<b>#metab</b>	<b>CNS</b>	<b>Qplog BB</b>
3-TFMPP	445.062	174.628	32.887	120.723	1	2	0.965
3-TFMBzPP	590.621	162.575	2.682	307.951	3	2	1.103

Table4.

<b>Compound</b>	<b>Mol wt</b>	<b>Donor HB</b>	<b>Accept HB</b>	<b>Logp</b>	<b>% Human oral absorption</b>	<b>Rule of 5</b>
3-TFMPP	230.232	1	2.5	2.611	3	0
3-TFMBzpp	320.357	0	3	4.725	3	0

Table 3&Table 4: Pharmacodynamic effects of 3-TFMPP and 3-TFMBzPP

## Computational analysis:

Table 5: Computational analysis for Alpha secretase

Compounds	Alpha secretase	
	Binding Affinity (reported in kcal/mol)	Docking Score
<b>Enhancer (Etazolate)</b>	-8.16	-3.9
<b>Inhibitor (Batimastat)</b>	-29.9	-4.9
<b>3-TFMPP</b>	7.48	-5.242
<b>3-TFMBzPP</b>	-8.64	-4.731

Table 6: Computational analysis for beta secretase

Compounds	Beta secretase	
	Binding Affinity (reported in kcal/mol)	Docking Score
<b>Enhancer (Talsaclidine)</b>	-23.9	-3.7
<b>Inhibitor Verubecestat (MK-8931)</b>	-53.3	-4.6
<b>3-TFMPP</b>	-32.6	-5.352
<b>3-TFMBzPP</b>	-32.2	-4.4

Table 7: Computational analysis for gamma secretase

Compounds	Gamma secretase	
	Binding Affinity (reported in kcal/mol)	Docking Score
<b>Natural ligand (APP)</b>	-73.61	-7.9
<b>Enhancer (Semagacestat)</b>	-36.5	-5.1
<b>Inhibitor (MRK 560)</b>	-44.1	-6.2
<b>3-TFMPP</b>	-29.32	-5.5
<b>3-TFMBzPP</b>	-43.7	-6.1

Molecular docking by utilizing structure-based drug design is used to predict the structures of the ligand-receptor complex, and it is particularly useful when finding new drugs or inhibitors to known enzymes or proteins associated with a given biological process. The main goal of this computational study is to determine the most favorable binding poses of hit compounds or ligand orientation within the active site of macromolecules such as enzymes and receptors. In addition, molecular mechanics generalized born surface area (MM/GBSA) is another commonly used technique to calculate the free binding energy and predict binding poses and affinities of ligands. First, we must point out the binding mode, affinity, and docking score of the natural ligands since they are preferred by the protein and have all the proper interactions that a potential inhibitor should replicate. (Ferreira, 2015)

### **III. Effect of TFMPP parent piperazine its structural derivative (3-TFMPP and 3-TFMBzPP) on Amyloid-beta ( $A\beta$ ) metabolism in PS70 cells**

1. Effect of parent piperazine drug its structural derivative (3-TFMPP and 3-TFMBzPP) on gamma ( $\gamma$ )-secretase activity in PS70 cells:

Dose-dependent effect of parent piperazine (3-TFMPP) and its derivative (3-TFMBzPP) was investigated on gamma ( $\gamma$ )-secretase activity using fluorometric method in the PS70 cells. Non-toxic doses of 3-TFMPP (100pM & 1nM) and 3-TFMBzPP (10nM & 1 $\mu$ M) on PS70 cells were used in the current study. Both the doses of 3-TFMPP (100pM & 1nM) did not affect the activity of gamma ( $\gamma$ )-secretase activity in the PS70 cells. However, 3-TFMBzPP (10nM = 35.5% & 1 $\mu$ M = 49.42%) dose-dependently and significantly inhibited the gamma ( $\gamma$ )-secretase activity in the PS70 cells (figure-6).



Figure 6: Effect of 3-TFMPP and 3-TFMBzPP on gamma secretase

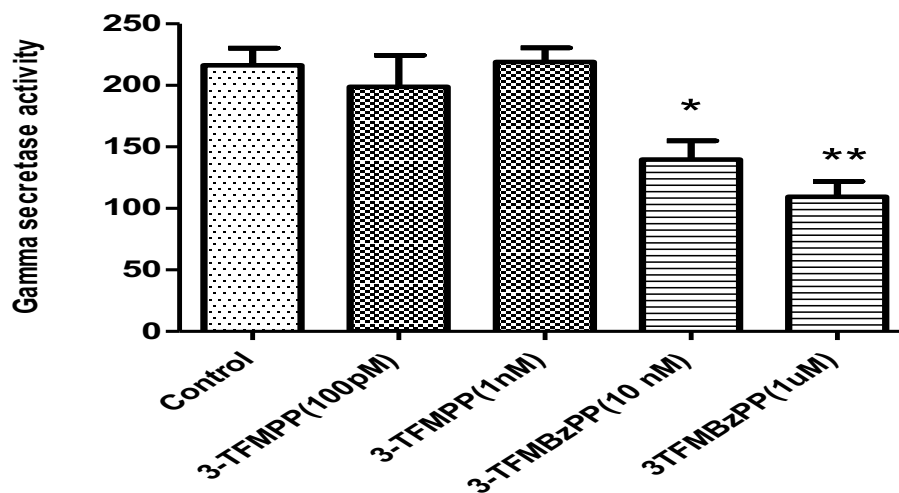


Figure-6: 3-TFMBzPP dose-dependently inhibited gamma ( $\gamma$ )-secretase activity in PS70 cells: PS70 transfected hamster ovarian cells were treated with different concentrations of 3-TFMPP (100pM & 1nM) and 3-TFMBzPP (10nM & 1 $\mu$ M) and incubated for 48 hours. Fluorometric assay procedure was used to evaluate the gamma ( $\gamma$ )-secretase activity using a specific substrate (NMA-GGVVIATVK(DNP)-DRDRDR-NH<sub>2</sub>). Results are expressed as fluorometric product formed/mg protein, Mean  $\pm$  SEM. 3-TFMBzPP (10nM & 1 $\mu$ M) dose-dependently and significantly inhibited the gamma ( $\gamma$ )-secretase activity as compared to the control (Figure-6, \* $p$  < 0.05).

2. Effect of parent piperazine drug its structural derivative (3-TFMPP and 3-TFMBzPP) on alpha ( $\alpha$ )-secretase activity in PS70 cells:

Dose-dependent effect of parent piperazine (3-TFMPP) and its derivative (3-TFMBzPP) was investigated on alpha ( $\alpha$ )-secretase activity using fluorometric method in the PS70 cells. Non-toxic doses of 3-TFMPP (100pM & 1nM) and 3-TFMBzPP (10nM & 1 $\mu$ M) on PS70 cells were

used in the current study. Both the doses of 3-TFMPP (100pM & 1nM) and 3-TFMBzPP (10nM & 1μM) did not affect the activity of alpha ( $\alpha$ )-secretase activity in the PS70 cells.

Figure 7:Effect of 3-TFMPP and 3-TFMBzPP on alpha secretase

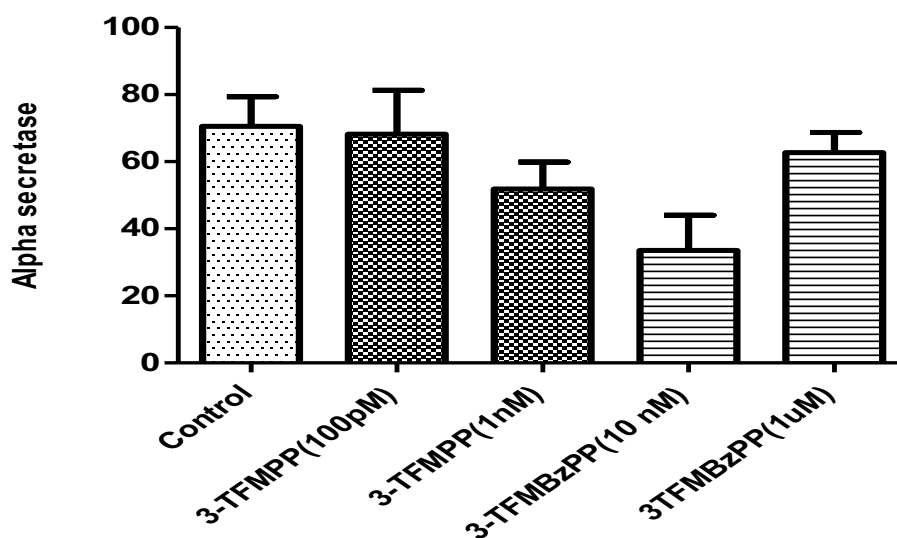


Figure-7: 3-TFMPP and 3-TFMBzPP did not affect the alpha ( $\alpha$ )-secretase activity in PS70 cells: PS70 transfected hamster ovarian cells were treated with different concentrations of 3-TFMPP (100pM & 1nM) and 3-TFMBzPP (10nM & 1μM) and incubated for 48hours. Fluorometric assay procedure was used to evaluate the alpha ( $\alpha$ )-secretase activity using a specific substrate (Ac-RE(EDANS)-VHHQKLVF-K(DABCYL)-R-OH). Results are expressed as fluorometric product formed/mg protein, Mean  $\pm$  SEM. 3-TFMPP (100pM & 1nM) and 3-TFMBzPP (10nM & 1μM) did not affect the alpha ( $\alpha$ )-secretase activity as compared to the control (Figure-,7)

3. Effect of parent piperazine drug its structural derivative (3-TFMPP and 3-TFMBzPP) on neprilysin activity in PS70 cells:

Dose-dependent effect of parent piperazine (3-TFMPP) and its derivative (3-TFMBzPP) was investigated on neprilysin activity using fluorometric method in the PS70 cells. Non-toxic doses of 3-TFMPP (100pM & 1nM) and 3-TFMBzPP (10nM & 1µM) on PS70 cells were used in the current study. Both the doses of 3-TFMPP (100pM & 1nM) and 3-TFMBzPP (10nM & 1µM) did not affect the activity of neprilysin activity.

Figure 8:Effect of 3-TFMPP and 3-TFMBzPP neprilysin activity

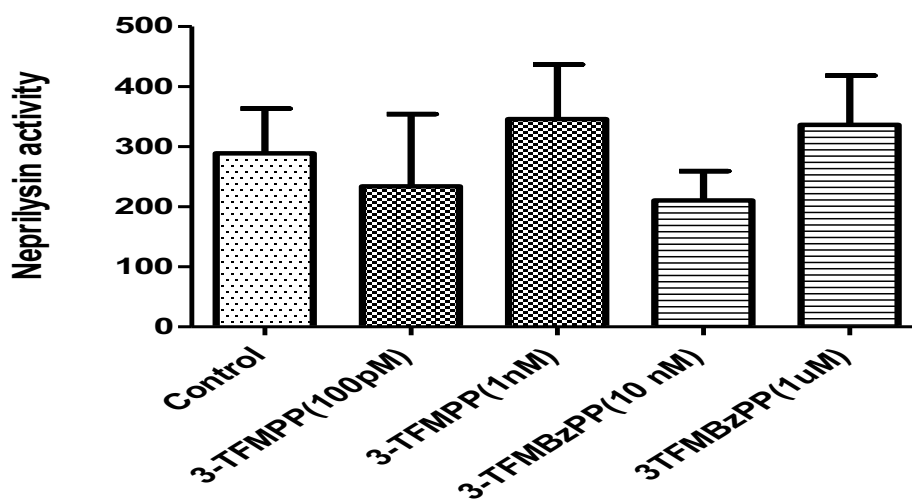


Figure-8: 3-TFMPP and 3-TFMBzPP did not affect the neprilysin activity in PS70 cells: PS70 transfected hamster ovarian cells were treated with different concentrations of 3-TFMPP (100pM & 1nM) and 3-TFMBzPP (10nM & 1µM) and incubated for 48hours. Fluorometric assay procedure was used to evaluate the neprilysin activity using neprilysin substrate. Results are expressed as fluorometric product formed/mg protein, Mean ± SEM. 3-TFMPP (100pM & 1nM) and 3-TFMBzPP (10nM & 1µM) did not affect the neprilysin activity as compared to the control (Figure-8,).

4. Effect of parent piperazine drug its structural derivative (3-TFMPP and 3-TFMBzPP) on amyloid-beta ( $A\beta$ )-42 content in PS70 cells:

Dose-dependent effect of parent piperazine (3-TFMPP) and its derivative (3-TFMBzPP) was investigated on extracellular amyloid-beta ( $A\beta$ )-42 content using commercial ELISA kit in the PS70 cells. Non-toxic doses of 3-TFMPP (100pM & 1nM) and 3-TFMBzPP (10nM & 1 $\mu$ M) on PS70 cells were used in the current study. Both the doses of 3-TFMPP (100pM & 1nM) did not affect the extracellular amyloid-beta ( $A\beta$ )-42 content in the PS70 cells. However, 3-TFMBzPP (10nM & 1 $\mu$ M) significantly decreased the extracellular amyloid-beta ( $A\beta$ )-42 content in the PS70 cells.

Figure 9: Effect of 3-TFMPP and 3-TFMBzPP on ( $A\beta$ )-42 content

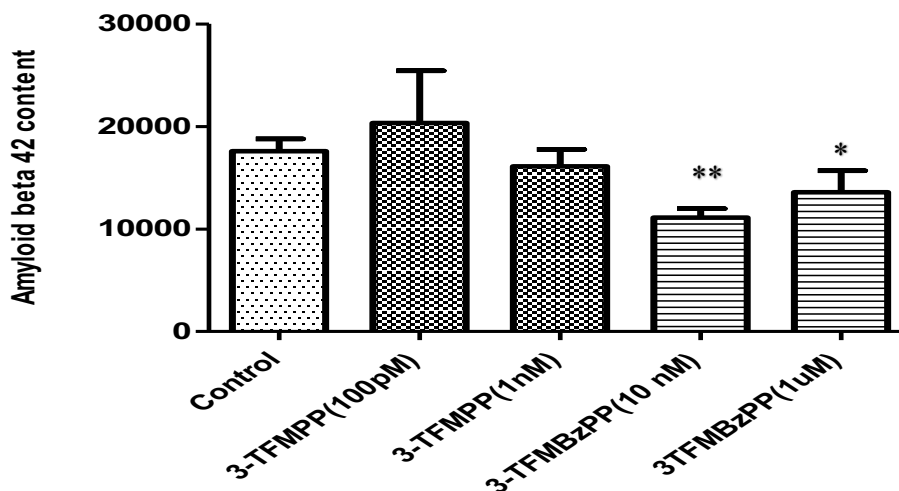


Figure-9: 3-TFMBzPP significantly decreased the extracellular amyloid-beta ( $A\beta$ )-42 in PS70 cells:

PS70 transfected hamster ovarian cells were treated with different concentrations of 3-TFMPP (100pM & 1nM) and 3-TFMBzPP (10nM & 1 $\mu$ M) and incubated for 48hours. Commercial ELISA kit was used to quantify the extracellular amyloid-beta ( $A\beta$ )-42 content. Results are expressed as Mean  $\pm$  SEM. 3-TFMBzPP (10nM & 1 $\mu$ M) significantly decreased the extracellular amyloid-beta ( $A\beta$ )-42 in PS70 cells as compared to the control (Figure-9, \* $p$  < 0.05)

5. Effect of parent piperazine drug its structural derivative (3-TFMPP and 3-TFMBzPP) on amyloid-beta (A $\beta$ )-42 expression in PS70 cells:

To further confirm, total amyloid-beta (A $\beta$ ) levels, western blots were performed. The results further confirmed that 3-TFMBzPP (1 $\mu$ M) significantly decreased total amyloid-beta (A $\beta$ )-42 expression (50%) in PS70 cells as compared to the control (Figure-10, \* $p < 0.05$ ).

Figure 10: Effect of 3-TFMPP and 3-TFMBzPP on (A $\beta$ )-42 expression

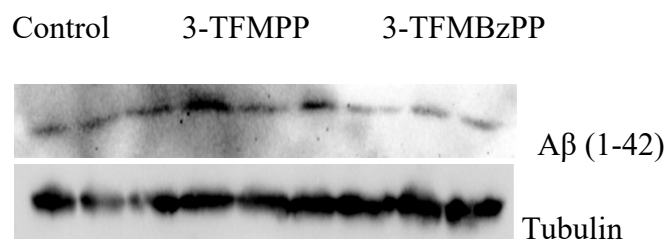
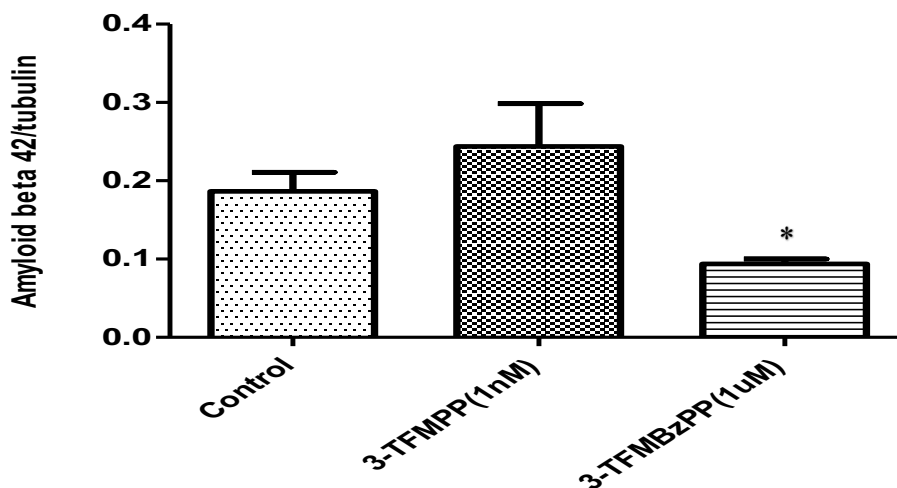


Figure 10: 3-TFMBzPP significantly decreased the amyloid-beta (A $\beta$ )-42 expression in PS70 cells:

PS70 transfected hamster ovarian cells were treated with 3-TFMPP and 3-TFMBzPP and incubated for 48hours. Western blot analysis was performed, and band intensity was normalized to the respective beta-tubulin. Results are expressed as Mean  $\pm$  SEM. 3-TFMBzPP (1 $\mu$ M) significantly reduced amyloid-beta (A $\beta$ )-42 expression in PS70 cells as compared to the control (Figure-10, \* $p < 0.05$ ).

6. Effect of parent piperazine drug its structural derivative (3-TFMPP and 3-TFMBzPP) on soluble amyloid precursor protein-alpha (sAPP $\alpha$ ) expression in PS70 cells:

Effect of 3-TFMPP and 3-TFMBzPP on soluble amyloid precursor protein-alpha (sAPP $\alpha$ ) expression in PS70 cells expression were studied using western blot. 3-TFMPP and 3-TFMBzPP did not affect the expression of the soluble amyloid precursor protein-alpha (sAPP $\alpha$ ) as compared to the control (Figure-11).

Figure 11: Effect of 3-TFMPP and 3-TFMBzPP on APP $\alpha$  expression

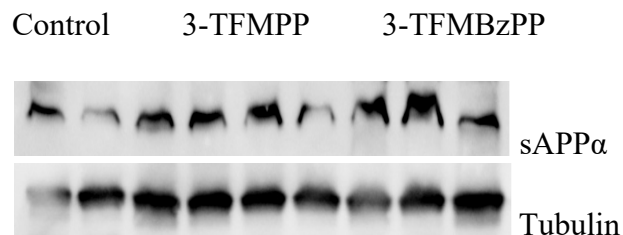
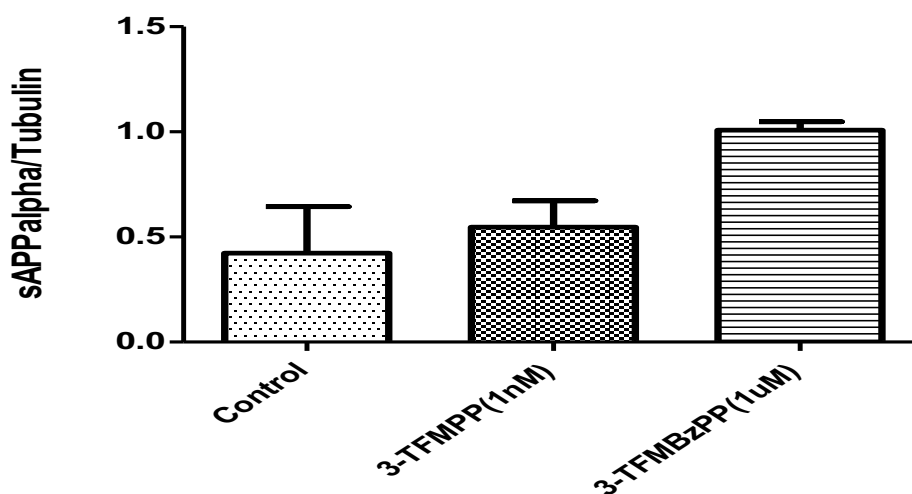


Figure 11: 3-TFMPP and 3-TFMBzPP did not affect the soluble amyloid precursor protein-alpha (sAPP $\alpha$ ) expression:

PS70 transfected hamster ovarian cells were treated with 3-TFMPP and 3-TFMBzPP and incubated for 48hours. Western blot analysis was performed, and band intensity was normalized to the respective beta-tubulin. Results are expressed as Mean  $\pm$  SEM. 3-TFMPP and 3-TFMBzPP did not affect the soluble amyloid precursor protein-alpha (sAPP $\alpha$ ) expression as compared to the control (figure 11).

7. Effect of parent piperazine drug its structural derivative (3-TFMPP and 3-TFMBzPP) on beta ( $\beta$ )-secretase expression (BACE) expression in PS70 cells:

Effect of 3-TFMPP and 3-TFMBzPP on the beta ( $\beta$ )-secretase expression (BACE) expression in PS70 cells were studied using western blot. 3-TFMPP and 3-TFMBzPP decreased the expression of the beta ( $\beta$ )-secretase expression (BACE) in significant manner as compared to the control (Figure-12).

Figure 12: Effect of 3-TFMPP and 3-TFMBzPP on beta secretase expression

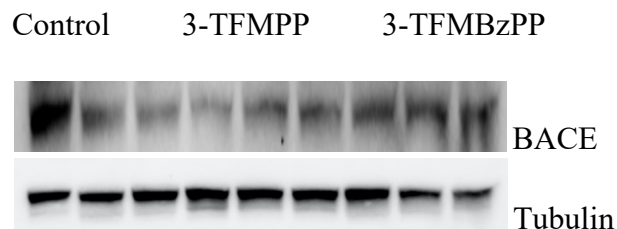
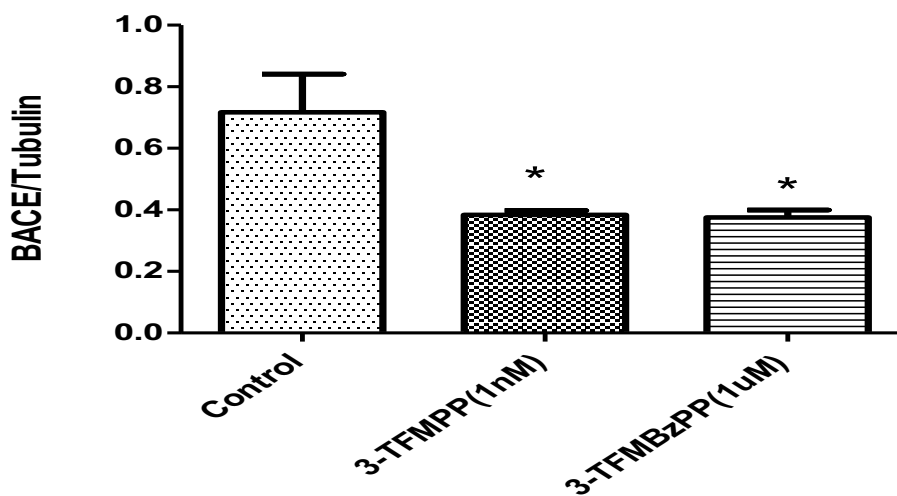


Figure-12: Effect of 3-TFMPP and 3-TFMBzPP on ( $\beta$ )-secretase expression: 3-TFMPP and 3-TFMBzPP significantly decreased the expression of the beta ( $\beta$ )-secretase expression (BACE) as compared to the control. PS70 transfected hamster ovarian cells were treated with 3-TFMPP and 3-TFMBzPP and incubated for 48 hours. Western blot analysis was performed, and band intensity was normalized to the respective beta-tubulin. Results are expressed as Mean  $\pm$  SEM. (Figure-12).

8. Effect of parent piperazine drug its structural derivative (3-TFMPP and 3-TFMBzPP) on total amyloid precursor protein (T-APP) expression in PS70 cells:

Effect of 3-TFMPP and 3-TFMBzPP on the total amyloid precursor protein (T-APP) expression in PS70 cells were studied using western blot. 3-TFMPP and 3-TFMBzPP did not effect on the expression of the total amyloid precursor protein (T-APP) expression as compared to the control (Figure-13)

Figure 13: Effect of 3-TFMPP and 3-TFMBzPP on total APP expression

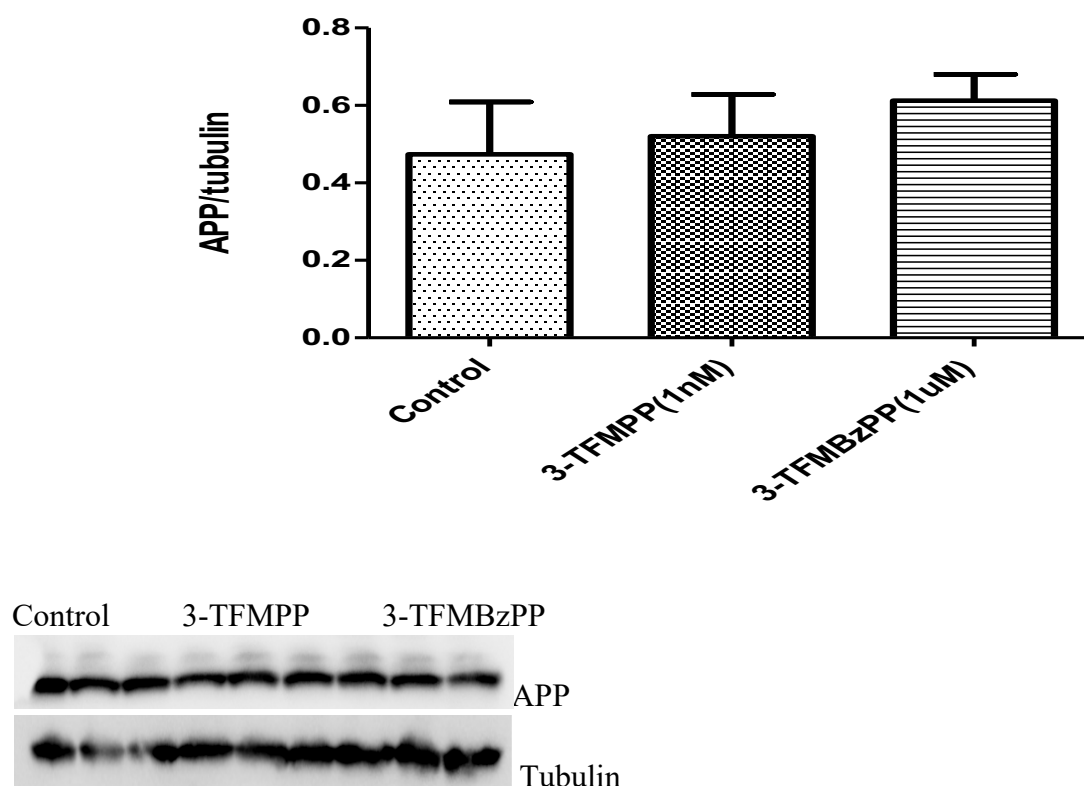


Figure-13: 3-TFMPP and 3-TFMBzPP on APP expression:

PS70 transfected hamster ovarian cells were treated with 3-TFMPP and 3-TFMBzPP and incubated for 48hours. 3-TFMPP and 3-TFMBzPP did not effect on the expression of the total amyloid precursor protein (T-APP) expression as compared to the control. Western blot analysis was performed, and band intensity was normalized to the respective beta-tubulin. Results are expressed as Mean ± SEM. (Figure-13)



#### **IV. Effect of piperazine designer drug and its derivative (3-TFMPP and 3-TFMBzPP) on various pro-oxidant markers in the PS70 cells:**

- a. Effect of piperazine designer drug and its derivative (3-TFMPP and 3-TFMBzPP) on reactive oxygen species (ROS) generation:

ROS generation in the control and different doses of piperazine designer drugs (3-TFMPP and 3-TFMBzPP) treated PS70 cells was measured based on the conversion of non-fluorescent substrate DCF (2',7'- Dichlorofluorescein diacetate) to the fluorescent product that was quantified spectrofluorometric ally. The generation of ROS were significantly increased in a dose-dependent manner in 3-TFMPP (1 $\mu$ M = 41.7%, 1mM = 247.3%) and 3-TFMBzPP (1 $\mu$ M = 144.1%, 1mM = 97.5%) treated cells as compared to the control. However, the parent drug (3-TFMPP) generated a significantly higher amount of ROS as compared to the control (Figure-14, \* $p < 0.05$ ,  $n = 5$ ).

- b. Effect of piperazine designer drug and its derivative (3-TFMPP and 3-TFMBzPP) on nitrite content:

Nitrite content in the control and different doses of piperazine designer drugs (3-TFMPP and 3-TFMBzPP) treated PS70 cells was quantified calorimetrically based on the formation of azo product by the nitrite content reacting with the Griess reagent. Similar to the ROS generation, nitrite content was significantly increased in a dose-dependent manner by 3-TFMPP (1mM = 157%) and 3-TFMBzPP (1mM = 50%) treated cells as compared to the control. However, the parent drug (3-TFMPP) generated a significantly higher amount of ROS as compared to the

control (Figure-15, ( $*p < 0.05$ ,  $n = 5$ ). The parent designer drug 3-TFMPP (high dose) had the most profound effect on the increase in the nitrite content.

c. Effect of piperazine designer drug and its derivative (3-TFMPP and 3-TFMBzPP) on hydrogen peroxide content.

Hydrogen peroxide content in the control and different doses of piperazine designer drugs (3-TFMPP and 3-TFMBzPP) treated cells was quantified fluorometrically. Parent designer drug, 3-TFMPP ( $1\mu\text{M} = 139.65\%$ ,  $1\text{mM} = 1678.5\%$ ) and its structural congener-3-TFMBzPP ( $1\mu\text{M} = 52.7\%$ ,  $1\text{mM} = 143.4\%$ ) dose-dependently induced substantial increased in hydrogen peroxide content compared to the control (Table-8,  $*p < 0.05$ ,  $n = 5$ ).

d. Effect of piperazine designer drug and its derivative (3-TFMPP and 3-TFMBzPP) on lipid peroxide content.

Lipid peroxide content in the control and different doses of piperazine designer drugs (3-TFMPP and 3-TFMBzPP) treated cells was measured calorimetrically based on the formation of thiobarbituric acid reactive substances (TBARS) by the reaction of lipid peroxides with the thiobarbituric acid. Due the increase in the prooxidants content (ROS, hydrogen peroxide and nitrite), the high dose of the parent designer drug (3-TFMPP,  $1\text{mM}$ ) induced significant increase in lipid peroxide content ( $297\%$ ) as compared to the control, while the low dose ( $1\mu\text{M}$ - $31\%$ ) and high dose ( $1\text{mM}$ - $77\%$ ) of 3TFMBzPP increased lipid peroxide content as compared to the control (figure-16,  $*p < 0.05$ ,  $n = 5$ ).

Figure 14: Effect of 3-TFMPP and 3-TFMBzPP on ROS generation

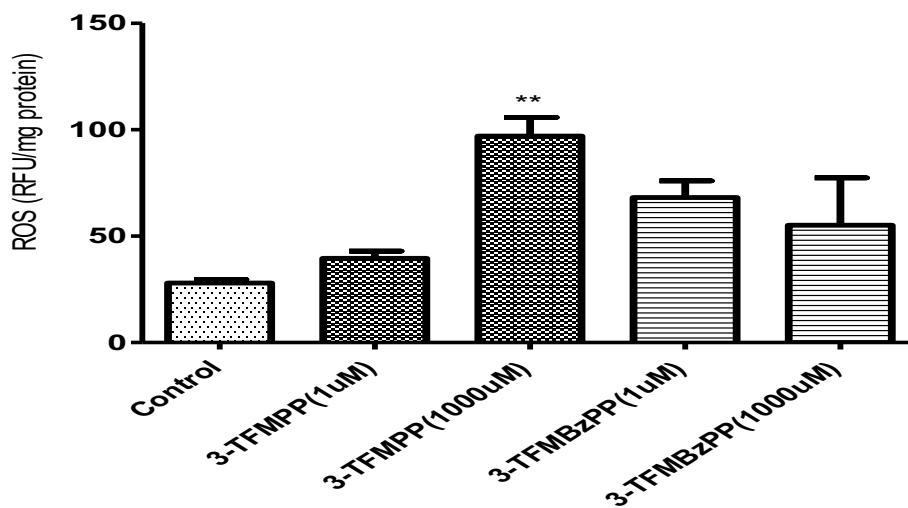


Figure-14: Reactive oxygen species was measured spectrofluorimetrically at (460nm / 528nm). Results are expressed as Mean  $\pm$  SEM, the relative fluorescence units/mg protein. 3-TFMPP (1000uM) induced a significant dose-dependent increase in reactive oxygen species generation as compared to the control ( $*p < 0.05$ ,  $n = 5$ ).

Figure 15: Effect of 3-TFMPP and 3-TFMBzPP on nitrite content

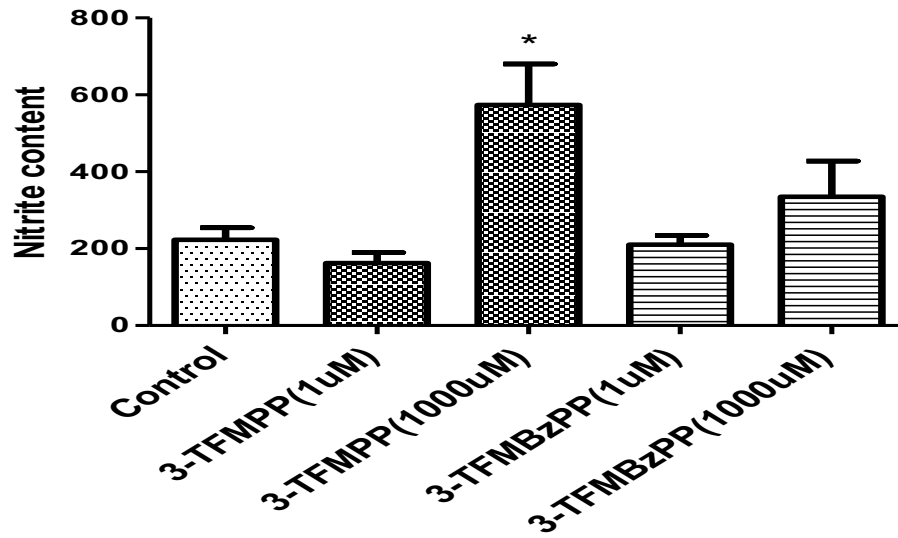


Figure-15: Nitrite content was measured spectrophotometrically at 540nm. Results are expressed as Mean  $\pm$  SEM, nitrite content  $\mu\text{M}/\text{mg}$  protein. 3-TFMPP (1000 $\mu\text{M}$ ) induced a significant dose-dependent increase in nitrite content as compared to the control (\* $p < 0.05$ ,  $n = 5$ ).

Figure 16: Effect of 3-TFMPP and 3-TFMBzPP on lipid peroxide content

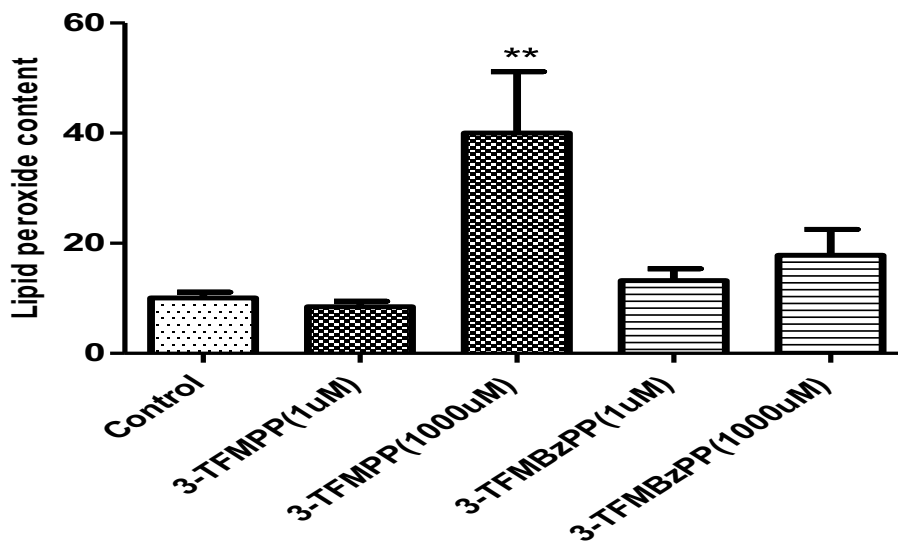


Figure-16: Lipid peroxide was measured spectrophotometrically (532nm). Results are expressed as Mean  $\pm$  SEM, TBARS content / mg protein. Due to the increased reactive oxygen species generation and nitrite content, 3-TFMPP induced a significant dose-dependent increased formation of lipid peroxide (as seen by the TBARS) as compared to the control (\* $p < 0.05$ ,  $n = 5$ ).

Table 8: Effect of 3-TFMPP and 3-TFMBzPP on Hydrogen peroxide content

	Hydrogen peroxide content ( $\mu\text{M}/\text{mg}$ protein)
Control	4792 + 445
3-TFMPP(1 $\mu\text{M}$ )	11484 $\pm$ 2044
3-TFMPP (1000 $\mu\text{M}$ )	85228 $\pm$ 25433**
3-TFMBzPP(1 $\mu\text{M}$ )	7317 $\pm$ 1700.7
3-TFMBzPP(1000 $\mu\text{M}$ )	11665 $\pm$ 1878.4

Table8: 3-TFMPP and 3-TFMBzPP induced dose dependent increase in hydrogen peroxide content as compared to the control. Results are expressed as Mean  $\pm$  SEM, (\* $p < 0.05$ ,  $n = 5$ ).

**V. Effect of piperazine designer drug and its derivative (3-TFMPP and 3-TFMBzPP) on various antioxidant markers in the PS70 cells:**

a. Effect of piperazine designer drug and its derivative (3-TFMPP and 3-TFMBzPP) on glutathione content:

Glutathione is a potent antioxidant molecule and structurally it is a simple tripeptide. Glutathione contains amino acids (Cysteine, glycine and glutamic acid) and cysteine is an amino acid with sulfhydryl group. This sulfhydryl group can undergo redox reaction and can scavenge toxic and active free radicals that can induce cellular damage. Glutathione content in the control and different doses of piperazine designer drugs (3-TFMPP and 3-TFMBzPP) treated cells was quantified spectrofluorimetrically based on the formation of OPT-condensation product by the reaction of glutathione with the OPT. Due the increase in the prooxidants content (ROS, hydrogen

peroxide and nitrite), the high dose of the parent designer drug (3-TFMPP, 1mM) induced significant depletion of glutathione content (78.2%) as compared to the control, while the low dose (1µM- 22.4%) and high dose (1mM-60.1%) of 3-TFMBzPP decreased glutathione content as compared to the control (figure-17, ( $*p < 0.05$ ,  $n = 5$ )).

Figure 17: Effect of 3-TFMPP and 3-TFMBzPP on glutathione content

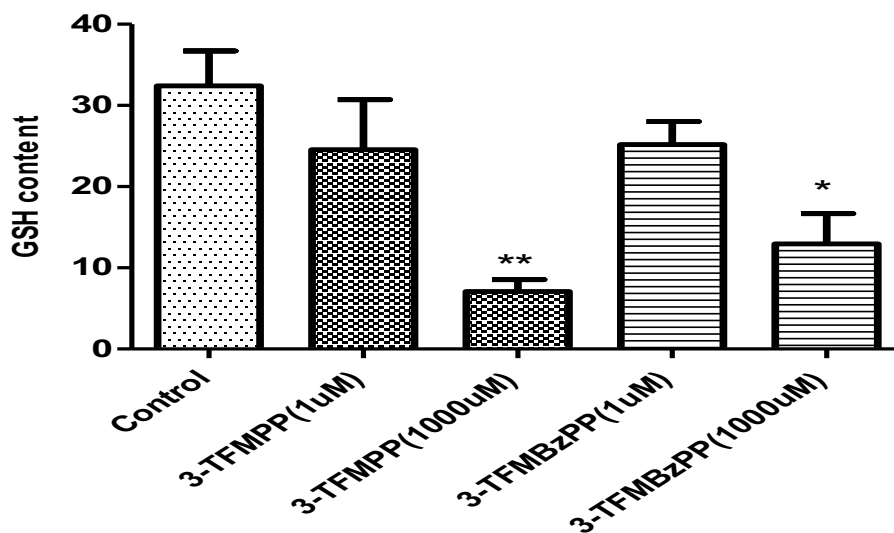


Figure-17: Glutathione content was measured spectrofluorimetrically at 334/432nm. Results are expressed as Mean ± SEM, glutathione content / mg protein. 3-TFMPP (1000uM), 3-TFMBzPP (1uM), and 3-TFMBzPP (1000uM), induced a significant dose-dependent depletion of glutathione as compared to the control ( $*p < 0.05$ ,  $n = 5$ ).

**VI. Effect of piperazine designer drug and its derivative (3-TFMPP and 3-TFMBzPP) on mitochondrial function in the PS70 cells:**

- a. Effect of piperazine designer drug and its derivative (3-TFMPP and 3-TFMBzPP) on mitochondrial Complex-I activity:

Mitochondrial Complex-I activity in the control and different doses of piperazine designer drugs (3-TFMPP and 3-TFMBzPP) treated cells was measured spectrophotometrically based on the oxidation of NADH at 340nm. 3-TFMPP induced dose-dependent decrease of the mitochondrial Complex-I activity (1 $\mu$ M = 76%, 1mM = 49%) as compared to the control. However, the piperazine derivative (3-TFMBzPP) did not affect the mitochondrial Complex-I activity as compared to the control (Figure-18, \* $p < 0.05$ ,  $n = 5$ ).



Figure 18: Effect of 3-TFMPP and 3-TFMBzPP on Complex-1 activity

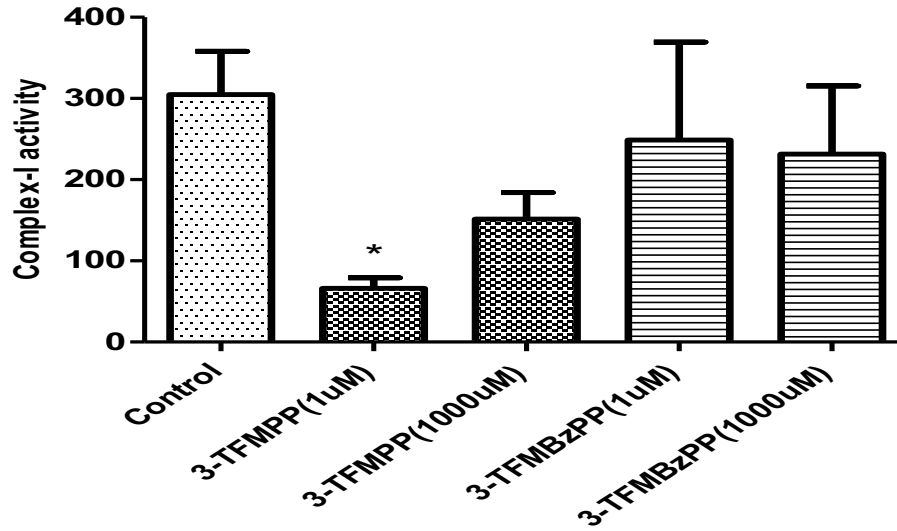


Figure-18: Mitochondrial Complex-I was measured spectrophotometrically (340nm). Results are expressed as Mean ± SEM, NADH content / mg protein. Mitochondrial Complex I activity was based on NADH oxidation, 3-TFMPP induced a significant dose-dependent decrease in mitochondria Complex-I activity (as seen by the NADH oxidation) as compared to the control (\*p < 0.05, n = 5).

Table 9: Effect of 3-TFMPP and 3-TFMBzPP on NADH content

Control	3-TFMPP (1uM)	3-TFMPP (1mM)	3-TFMBzPP (1uM)	3-TFMBzPP (1mM)
1343 ± 354.7	861.1 ± 288.7	1811 ± 325.5	1401 ± 485.6	958.6 ± 355.8

Table9: 3-TFMPP and 3-TFMBzPP did not affect the NADH content as compared to the control. Results are expressed as Mean ± SEM, n =5,

**VII. Effect of piperazine designer drug and its derivative (3-TFMPP and 3-TFMBzPP) on inflammatory markers in the PS70 ovarian cells:**

a. Effect of piperazine designer drug and its derivative (3-TFMPP and 3-TFMBzPP) on cyclooxygenase activity:

Cyclooxygenase activity in the control and different doses of piperazine designer drugs (3-TFMPP and 3-TFMBzPP) treated cells was quantified calorimetrically at 600nm by using TMPD as substrate. Cyclooxygenase cleaved TMPD substrate and the product that formed from cleavage of the TMPD substrate was quantified calorimetrically. 3-TFMPP induced dose-dependent increase of the cyclooxygenase activity (1mM = 574.7%) as compared to the control. The parent designer drug 3-TFMPP (high dose) had the most profound effect on the increase in the cyclooxygenase activity (figure 19).

b. Effect of piperazine designer drug and its derivative (3-TFMPP and 3-TFMBzPP) on caspase-1 activity:

Caspase-1 activity in the control and different doses of piperazine designer drugs (3-TFMPP and 3-TFMBzPP) treated cells was quantified using AC-DEVD-AMC as substrate and formed product was measured fluorometrically at 360/460nm. Caspase-1 activates the inactive pro-IL-1 $\beta$  by cleaving at YVHD (119)-A and this produces bioactive IL-1 $\beta$ . 3-TFMPP and 3-TFMBzPP induced dose-dependent non-significant increase of the caspase-1 activity (1mM = 69%) and as compared to the control. The piperazine derivative (3-TFMBzPP) non significantly increased the caspase-1 activity as compared to the control (Table 10, n = 5).

Figure 19: Effect of 3-TFMPP and 3-TFMBzPP on cyclooxygenase activity

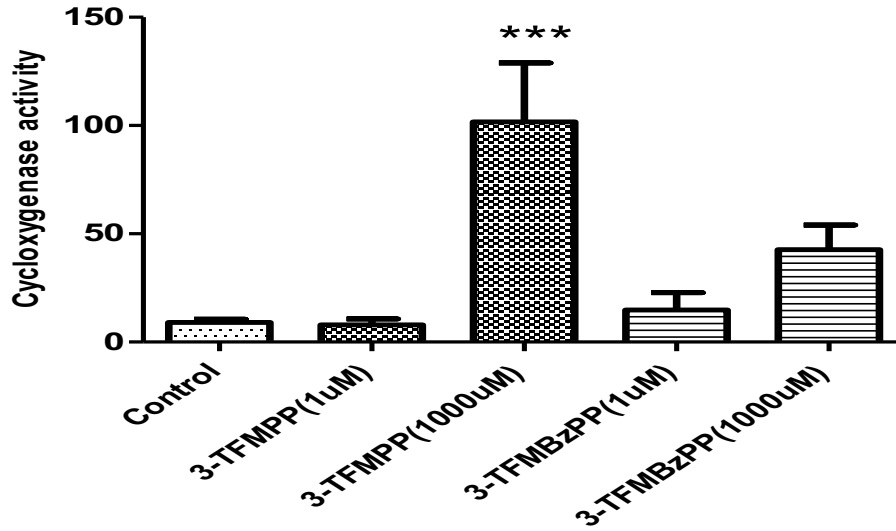


Figure19: Cyclooxygenase activity was measured calorimetrically (600nm). Results are expressed as Mean  $\pm$  SEM, TMPD metabolized / mg protein. Cyclooxygenase activity was based on TMPD metabolism by cyclooxygenase. 3-TFMPP induced a significant dose-dependent increase in cyclooxygenase activity as compared to the control (Figure-6,  $*p < 0.05$ ,  $n = 5$ ).

Table 10: Effect of 3-TFMPP and 3-TFMBzPP on Caspase 1 activity

Control	3-TFMPP (1uM)	3-TFMPP (1mM)	3-TFMBzPP (1uM)	3-TFMBzPP (1mM)
10.35 $\pm$ 1.29	13.76 $\pm$ 1.93	17.49 $\pm$ 3.01	13.02 $\pm$ 1.88	18.06 $\pm$ 355.8

Table-10: 3-TFMPP and 3-TFMBzPP non significantly increased caspase-1 as compared to the control. Results are expressed as Mean  $\pm$  SEM,  $n = 5$ ,

### **VIII. Effect of piperazine designer drug and its derivative (3-TFMPP and 3-TFMBzPP) on apoptosis markers in the PS70 cells:**

a. Effect of piperazine designer drug and its derivative (3-TFMPP and 3-TFMBzPP) on caspase-3 activity:

Caspase-3 (apopain, CPP-32, and Yama) is a cysteine protease that is activated initially in a sequence of signaling linked with apoptosis (programed cell death). Caspase-3 plays an important part in the apoptotic signaling by involving in the execution-phase through poly-(ADP)-ribose-polymerase cleavage. Furthermore, caspase 3 activates caspases 6, 7 and 9, and is itself processed by caspases 8, 9 and 10. Caspase-3 activity in the control and different doses of piperazine designer drugs (3-TFMPP and 3-TFMBzPP) treated cells was quantified using AC-DEVD-AMC as substrate and formed product was measured fluorometrically at 360/460nm. 3-TFMPP (1mM = 280%) induced significantly increased of the caspase-3 activity as compared to the control (Figure-20, n = 5).

b. Effect of piperazine designer drug and its derivative (3-TFMPP and 3-TFMBzPP) on caspase-8 activity:

Caspase-8 activity in the control and different doses of piperazine designer drugs (3-TFMPP and 3-TFMBzPP) treated cells was quantified using Ac-IETD-AMC as substrate and formed product was measured fluorometrically at 360/460nm. 3-TFMPP induced dose-dependent significant increase of the caspase-8 activity (1mM = 272.6%) as compared to the control. The piperazine derivative (3-TFMBzPP) did not have any effect on the caspase-8 activity as compared to the control. (Figure-21 b, n = 5).

c. Effect of piperazine designer drug and its derivative (3-TFMPP and 3-TFMBzPP) on caspase-9 activity:

Caspase-9 activity in the control and different doses of piperazine designer drugs (3-TFMPP and 3-TFMBzPP) treated cells was quantified using Ac-LEHD-AMC as substrate and formed product was measured fluorometrically at 360/460nm. 3-TFMPP induced dose-dependent significant increase of the caspase-9 activity (1mM = 242.65%) as compared to the control. The piperazine derivative (3-TFMBzPP) did not have any effect on the caspase-9 activity as compared to the control. (Figure-22, n = 5).

d. Effect of piperazine designer drug and its derivative (3-TFMPP and 3-TFMBzPP) on protease activity:

Protease activity in the control and different doses of piperazine designer drugs (3-TFMPP and 3-TFMBzPP) treated cells was quantified using Z-Gly-Gly-Leu-7-amido-4-methylcoumarin (Z-Gly-Gly-Leu-AMC) as substrate and formed product was measured fluorometrically at 380/440nm. 3-TFMPP induced dose-dependent significant decrease of the protease activity (1mM = 69%) as compared to the control. The piperazine derivative (3-TFMBzPP) did not have any effect on the protease activity as compared to the control (figure-23, n=5).

Figure 20: Effect of 3-TFMPP and 3-TFMBzPP on caspase 3 activity

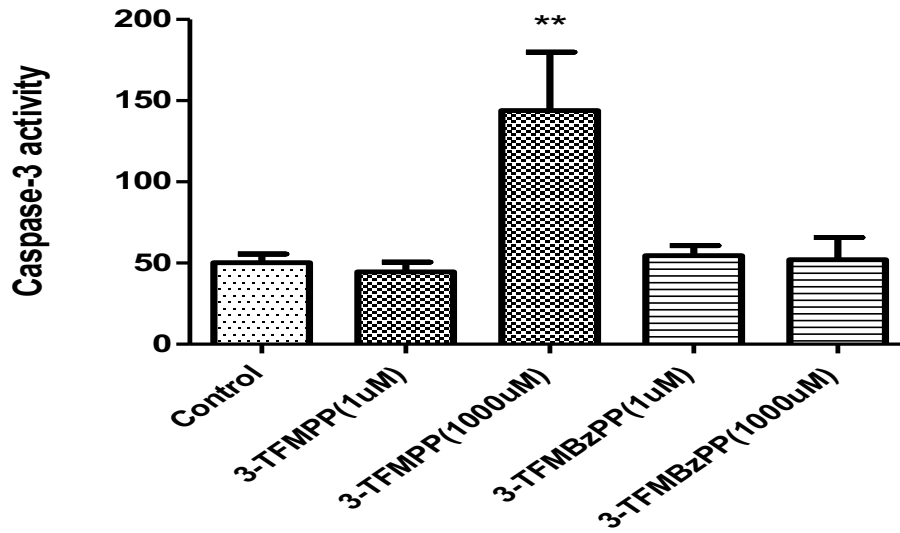


Figure-20: Caspase-3 activity was measured fluorometrically (360/460nm). Results are expressed as Mean  $\pm$  SEM, AMC formed / mg protein. Caspase-3 activity was based on AC-DEVD-AMC cleaved by Caspase-3. 3-TFMPP (1mM) induced a significant dose-dependent increase in caspase-3 activity as compared to the control (Figure-20,  $*p < 0.05$ ,  $n = 5$ ).

Figure 21: 3-TFMPP and 3-TFMBzPP on caspase8 activity

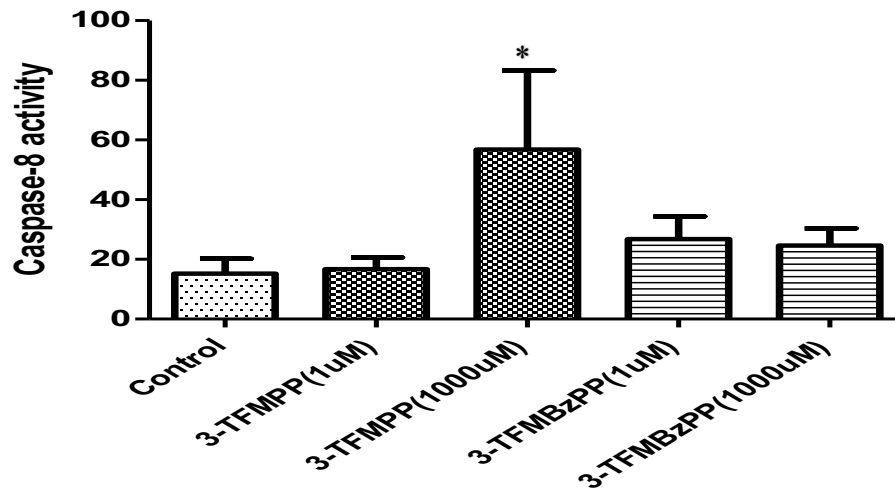


Figure-21: Caspase-8 activity was measured fluorometrically (360/460nm). Results are expressed as Mean  $\pm$  SEM, AMC formed / mg protein. Caspase-8 activity was based on Ac-IETD-AMC cleaved by Caspase8. 3-TFMPP (1mM) and 3-TFMBzPP (1mM) induced a significant dose-dependent increase in capase-8 activity as compared to the control (Figure-21, \* $p < 0.05$ , n = 5).

Figure 22: 3-TFMPP and 3-TFMBzPP on caspase 9 activity

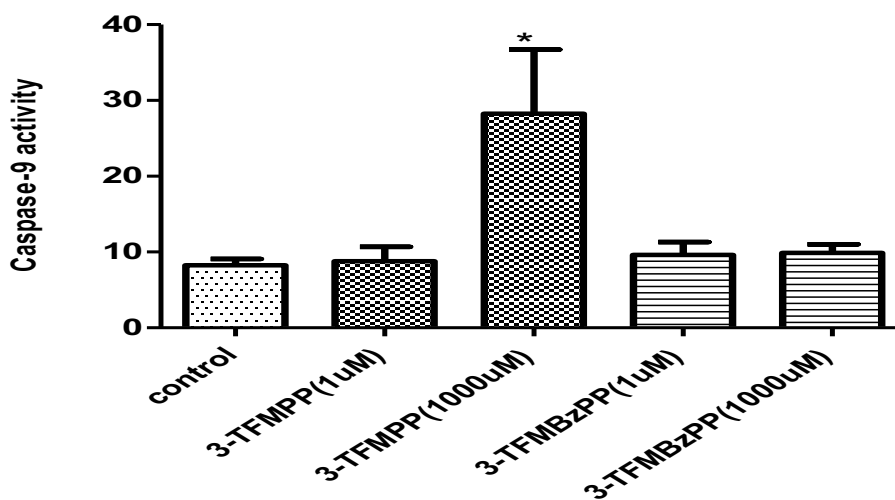


Figure-22: Caspase-9 activity was measured fluorometrically (360/460nm). Results are expressed as Mean  $\pm$  SEM, AMC formed / mg protein. Caspase-9 activity was based on Ac-LEHD-AMC cleaved by Caspase-9. 3-TFMPP (1mM) induced a significant increase in caspase-9 activity as compared to the control (Figure-22, \* $p < 0.05$ ,  $n = 5$ ).



Figure 23: 3-TFMPP and 3-TFMBzPP on protease activity

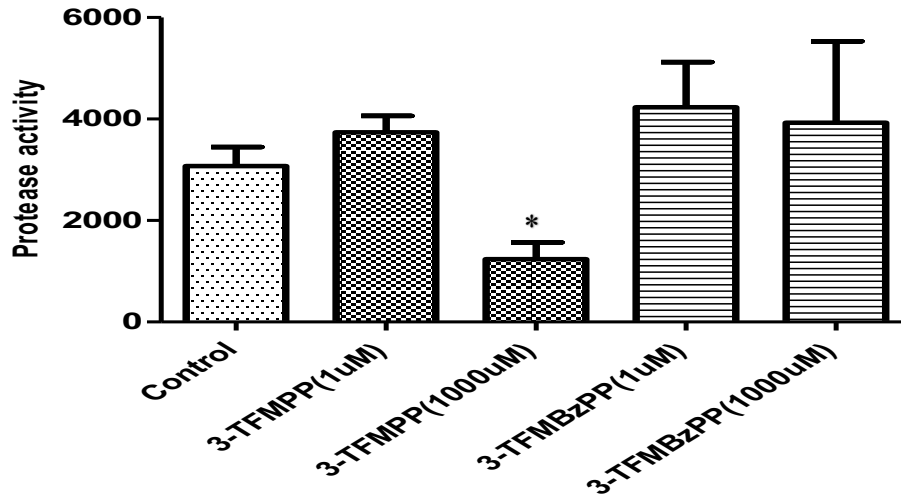
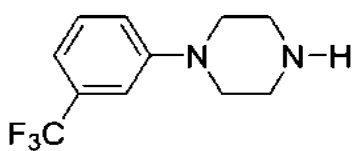
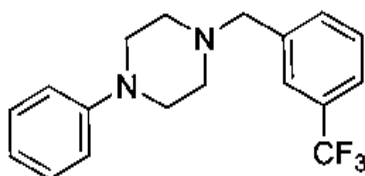


Figure-23: Protease activity was measured fluorometrically (380/440nm). Results are expressed as Mean  $\pm$  SEM, AMC formed / mg protein. Protease activity was based on using Z-Gly-Gly-Leu-7-amido-4-methylcoumarin (Z-Gly-Gly-Leu-AMC) = 5) substrate cleaved by protease. 3-TFMPP (1000 uM) significantly decreased the protease activity as compared to the control, (Figure-23, \* $p < 0.05$ ,  $n = 5$ ).

## Discussion



**3-TFMPP**



**3-TFMBzPP**

Consuming designer drugs have become a prevalence way to bring pleasure especially among young people. Piperazine compounds are from the most common designer drugs. In this study piperazine drugs (3-TFMPP and 3-TFMBzPP) were used to assess their neuroprotective effects on PS70 ovarian cells. PS70 cells is a valid *in vitro* model to study A $\beta$  pathology. In this study, we report that 3-TFMPP piperazine compound, in dose dependent manner increased generation of prooxidants (ROS and RNS) and decreased the antioxidant (glutathione). Imbalance between prooxidants and antioxidants, which is called oxidative stress was observed in 3-TFMP. Increase generation of ROS and nitrite species destroys cellular protein, carbohydrate, lipids, and nucleic acid leading to cellular damage throughout aging (Thapa et al. 2017). Accumulation of A $\beta$  in the brain is sign of AD (Hardy & Selkoe 2003). Metal ions such as copper, zinc and iron are essential to regulate the neuronal activity. However, in Alzheimer's disease the level of the metal ions exceeded the physiological level of the normal individual (Kozlowski et al., 2012). A $\beta$  contain high concentration of metal ions that involved in ROS production (Cheignon et al., 2018). It has been known that oxidative stress occurs at a very early stage of Alzheimer's disease even before A $\beta$  plaque formation and start of the symptoms (Nunomuea et al., 2001). Numerous cellular changes induced by oxidative damage have been correlated with A $\beta$  formation and pathological conditions of Alzheimer's disease (Anekonda et al., 2005). Elevation of ROS production and decrease in the antioxidant defense mechanism contributes to neurodegeneration caused by

oxidative stress (Gemma et al., 2007). Because increased reactive oxygen species generation and nitrite content, 3-TFMPP induced significant increase in formation of lipid peroxide. Exposure of poly unsaturated fatty acid to ROS leads to formation lipid peroxidation.

Mitochondria, a cytoplasmic organelle, are responsible for supply of energy to cells. Also, they regulate several cellular processes including apoptosis, cell cycle, ROS generation, and thermogenesis. Mitochondrial dysfunction is a key feature of neurodegenerative disorders including Alzheimer's disease (Hroudová et al., 2014). Complex-I, the largest enzyme of electron transport chain, is critical for cellular energy. Complex-1 oxidizes NADH to NAD<sup>+</sup>. In this study, we report that 3-TFMPP induced significant depletion in complex-I activity.

Neuronal loss is a feature of AD, and some researchers have hypothesized that dysregulation of apoptosis pathways is responsible for AD (Roth K., 2001). Apoptosis is regulated by caspases. Caspase enzymes are divided into two class interleukin 1beta converting enzyme (ICE)-1 like, and CED-3-like (Nicholson, D., 2000). CED-3 like caspase, which directly are involved in apoptosis, are classified into initiator caspases (Caspase 2, caspase 8, caspase 9 and caspase 10) and downstream effector caspase (caspase 3, caspase 6 and caspase 7). However, ICE like caspases (Caspase 1, caspase 4, caspase 5, and caspase 12) are implicated in the proteolytic processing of cytokines (Roth K., 2001). 3-TFMPP(1mM) significantly increased caspase 3 activ caspase 8 and caspase 9 activities, while 3-TFMBzPP didn't have any effects on caspases as compared to the control.

Soluble A $\beta$  stimulates activation of the proinflammatory component of primary microglia (Sondag, C et al., 2009). It also increases the secretion of proinflammatory cytokines such as nitric oxide, TNF $\alpha$ , and TNF $\beta$  (White, J et al., 2005). Accumulation of A $\beta$  leads to activation of microglia causing phagocytosis of A $\beta$  (Belmont, T et al., 2008). Nonetheless, sustained activation

of the immune response has been shown to contribute to an exacerbation of Alzheimer's disease pathology, possibly due to continued activation of microglia in a feed forward loop, called reactive microgliosis (Hickman, S et al., 2008 and Meda, L et al., 1995). Several proinflammatory cytokines are involved in Alzheimer's disease such as TNF- $\alpha$ , IL-1 $\beta$ , IL-6, and NF $\kappa$ B. To assess the effect of 3-TFMPP and 3-TFMBzPP on inflammation, ICE-1 and cyclooxygenase activities were measured. The high dose of 3-TFMPP induced significant increase in cyclooxygenase activity, while 3-TFMBzPP did not have any effects on cyclooxygenase. In this study we investigate that 3-TFMPP, exhibited higher toxic effects due to the increased generation of pro-oxidants and decreased antioxidants, enhanced apoptosis and inflammatory markers as compared to 3-TFMBzPP.

Computational modelling and receptor binding assay can envisage the pharmacokinetic and pharmacodynamic effects of parent piperazine (3-TFMPP) and its structural derivative (3-TFMBzPP). 3-TFMPP and 3-TFMBzPP, based on Lipinski's rule of five, Jorgensen's rule of three, QPlogBB and the QPPCaco, the TFMPP derivatives can undergo passive diffusion and can be highly absorbed after oral administration (can be bioactive orally). PISA and FOSA values can be used to correlate with the neurotoxicity of a drug / chemical. 3-TFMBzPP has lower SASA, FISA and FOSA values. Based on the CNS and Qlog values both the piperazine designer drugs can cross the BBB and possibly exhibit significant neuropharmacological effects in the central nervous system. 3-TFMBzPP exhibited significantly lower toxicity as compared to the TFMPP, the parent compound. Thus, the structural changes between the parent and its derivative can lead to change (increase / decrease) in potency or toxicity. The change in structure can cause more stimulatory, addictive, and toxic than their parent compound (stimulants / drugs of abuse). However, there is a possibility that these designer drugs can become less toxic and still exhibit the

required pharmacodynamic effects compared to the parent compounds. Thus, the non-toxic piperazine designer drugs can exhibit potent therapeutic effects to treat various ailments in humans and veterinary purposes.

In this study, we used specific drugs that enhances or inhibits the major enzymes associated with amyloid beta amyloid metabolism. With regard to the alpha-secretase activity, the binding affinity of 3-TFMBzPP was similar to the alpha-secretase enhancer (Etazolate). However, the effect of 3-TFMBzPP on gamma secretase was similar to the inhibitor of gamma secretase (MRK 560). Like the effect on gamma secretase, 3-TFMBzPP's effect on beta secretase was more closely resembling to its inhibitor, Verubecestat (MK-8931). Based on this observation, 3-TFMBzPP can significantly inhibit the synthesis and increase the clearance of Amyloid beta.

Pathologically, Alzheimer's disease is characterized by abnormal accumulation of extracellular A $\beta$  plaques and intracellular neurofibrillary tangles composed of hyperphosphorylated tau protein (Bayer, T. A., & Wirths, O., 2010).

The extracellular senile plaques that accumulate in the brain of Alzheimer's patients are caused by A $\beta$  through sequential cleavages of APP by  $\beta$  and  $\gamma$ -secretase. In this study, we also investigated the effect of the parent compound and its structural derivatives on A $\beta$  metabolism. We used no-toxic doses of 3-TFMPP and 3-TFMBzPP. Interestingly, 3-TFMBzPP induced significant inhibition of beta and gamma secretase activity. Also, 3-TFMBzPP significantly decreased content and expression of A $\beta$ 42. However, 3-TFMPP and 3-TFMBzPP did not have effect on the expression total APP. The effect of 3-TFMBzPP on A $\beta$ 42 was similar to the effect of the well-known stimulant, caffeine. Rat primary cerebral cortical neurons treated with LDL cholesterol significantly induced A $\beta$ 1–40 and A $\beta$ 1–42 formation. Interestingly, pretreatment with

caffeine (200 $\mu$ M for 24 h) significantly inhibited the A $\beta$ 1–40 and A $\beta$ 1–42 levels (Li Shanshan et al. 2015). Moreover, our drug 3-TFMBzPP (1  $\mu$ M) significantly reduced amyloid beta levels.

Thus, the piperazine designer drugs can be used as a neuroprotectant in a low dose. In future, we plan to investigate the *in vivo* neuroprotective effects of piperazine derivatives in a valid animal model of Alzheimer' disease.

#### **References:**

1. Chen, G.-F., Xu, T.-H., Yan, Y., Zhou, Y.-R., Jiang, Y., Melcher, K., & Xu, H. E. (2017). Amyloid beta: structure, biology and structure-based therapeutic development. *Acta Pharmacologica Sinica*, 38(9), 1205–1235. doi: 10.1038/aps.2017.28

2. Guerreiro, R. J., Gustafson, D. R., & Hardy, J. (2012). The genetic architecture of Alzheimer's disease: beyond APP, PSENs and APOE. *Neurobiology of aging*, 33(3), 437-456.
3. Wan, H., Lee, K. S., Kim, B. Y., Zou, F. M., Yoon, H. J., Je, Y. H., ... Jin, B. R. (2013). A spider-derived Kunitz-type serine protease inhibitor that acts as a plasmin inhibitor and an elastase inhibitor. *PloS one*, 8(1), e53343. doi: 10.1371/journal.pone.0053343
4. Jiang, S., Li, Y., Zhang, X., Bu, G., Xu, H., & Zhang, Y. W. (2014). Trafficking regulation of proteins in Alzheimer's disease. *Molecular neurodegeneration*, 9(1), 6.
5. Mattson, M. P. (2004). Pathways towards and away from Alzheimer's disease. *Nature*, 430(7000), 631-639.
6. Chow, V. W., Mattson, M. P., Wong, P. C., & Gleichmann, M. (2010). An overview of APP processing enzymes and products. *Neuromolecular medicine*, 12(1), 1-12.
7. Zheng, H., & Koo, E. H. (2011). Biology and pathophysiology of the amyloid precursor protein. *Molecular neurodegeneration*, 6(1), 27
8. Ozaki, T., Li, Y., Kikuchi, H., Tomita, T., Iwatsubo, T., & Nakagawara, A. (2006). The intracellular domain of the amyloid precursor protein (AICD) enhances the p53-mediated apoptosis. *Biochemical and biophysical research communications*, 351(1), 57-63
9. Saido, T., & Leissring, M. A. (2012). Proteolytic degradation of amyloid  $\beta$ -protein. *Cold Spring Harbor perspectives in medicine*, 2(6), a006379. doi:10.1101/cshperspect. a006379
10. Baranello, R. J., Bharani, K. L., Padmaraju, V., Chopra, N., Lahiri, D. K., Greig, N. H., ... Sambamurti, K. (2015). Amyloid-beta protein clearance and degradation (ABCD) pathways and their role in Alzheimer's disease. *Current Alzheimer research*, 12(1), 32-46. doi:10.2174/1567205012666141218140953

11. Iwata, N., Tsubuki, S., Takaki, Y., Shirotani, K., Lu, B., Gerard, N. P., ... & Saido, T. C. (2001). Metabolic regulation of brain A $\beta$  by neprilysin. *Science*, 292(5521), 1550-1552.
12. Iwata, N., Higuchi, M., & Saido, T. C. (2005). Metabolism of amyloid- $\beta$  peptide and Alzheimer's disease. *Pharmacology & therapeutics*, 108(2), 129-148.
13. Palmer, J. C., Baig, S., Kehoe, P. G., & Love, S. (2009). Endothelin-converting enzyme-2 is increased in Alzheimer's disease and up-regulated by A $\beta$ . *The American journal of pathology*, 175(1), 262-270.
14. Emoto, N., & Yanagisawa, M. (1995). Endothelin-converting enzyme-2 is a membrane-bound, phosphoramidon-sensitive metalloprotease with acidic pH optimum. *Journal of Biological Chemistry*, 270(25), 15262-15268.
15. Chen, G. F., Xu, T. H., Yan, Y., Zhou, Y. R., Jiang, Y., Melcher, K., & Xu, H. E. (2017). Amyloid beta: structure, biology and structure-based therapeutic development. *Acta Pharmacologica Sinica*, 38(9), 1205-1235.
16. Eckman, E. A., Reed, D. K., & Eckman, C. B. (2001). Degradation of the Alzheimer's amyloid  $\beta$  peptide by endothelin-converting enzyme. *Journal of Biological chemistry*, 276(27), 24540-24548.
17. SCHWEIZER, A., VALDENNAIRE, O., NELBÖCK, P., DEUSCHLE, U., DUMAS MILNE EDWARDS, J. B., STUMPF, J. G., & LÖFFLER, B. M. (1997). Human endothelin-converting enzyme (ECE-1): three isoforms with distinct subcellular localizations. *Biochemical Journal*, 328(3), 871-877.
18. Pacheco-Quinto, J., & Eckman, E. A. (2013). Endothelin-converting enzymes degrade intracellular  $\beta$ -amyloid produced within the endosomal/lysosomal pathway and autophagosomes. *Journal of Biological Chemistry*, 288(8), 5606-5615.



19. Farris, W., Mansourian, S., Chang, Y., Lindsley, L., Eckman, E. A., Frosch, M. P., ... & Guénette, S. (2003). Insulin-degrading enzyme regulates the levels of insulin, amyloid  $\beta$ -protein, and the  $\beta$ -amyloid precursor protein intracellular domain in vivo. *Proceedings of the National Academy of Sciences*, 100(7), 4162-4167.
20. Bertram, L., Blacker, D., Mullin, K., Keeney, D., Jones, J., Basu, S., ... & Selkoe, D. J. (2000). Evidence for genetic linkage of Alzheimer's disease to chromosome 10q. *Science*, 290(5500), 2302-2303.
21. Puthuchery, Z., Skipworth, J. R., Rawal, J., Loosemore, M., Van Someren, K., & Montgomery, H. E. (2011). The ACE gene and human performance. *Sports medicine*, 41(6), 433-448.
22. Hemming, M. L., & Selkoe, D. J. (2005). Amyloid  $\beta$ -protein is degraded by cellular angiotensin-converting enzyme (ACE) and elevated by an ACE inhibitor. *Journal of Biological Chemistry*, 280(45), 37644-37650.
23. Jacobsen, J. S., Comery, T. A., Martone, R. L., Elokdah, H., Crandall, D. L., Oganessian, A., ... & Zhou, H. (2008). Enhanced clearance of A $\beta$  in brain by sustaining the plasmin proteolysis cascade. *Proceedings of the National Academy of Sciences*, 105(25), 8754-8759.
24. Ries, M., & Sastre, M. (2016). Mechanisms of A $\beta$  clearance and degradation by glial cells. *Frontiers in aging neuroscience*, 8, 160.
25. Giuffrida, M. L., Caraci, F., De Bona, P., Pappalardo, G., Nicoletti, F., Rizzarelli, E., & Copani, A. (2010). The monomer state of beta-amyloid: where the Alzheimer's disease protein meets physiology. *Reviews in the neurosciences*, 21(2), 83-94.

26. Giuffrida, M. L., Caraci, F., Pignataro, B., Cataldo, S., De Bona, P., Bruno, V., ... & Garozzo, D. (2009).  $\beta$ -amyloid monomers are neuroprotective. *Journal of Neuroscience*, 29(34), 10582-10587.
27. Ow, S. Y., & Dunstan, D. E. (2014). A brief overview of amyloids and Alzheimer's disease. *Protein Science*, 23(10), 1315-1331.
28. Bishop, G. M., & Robinson, S. R. (2004). Physiological roles of amyloid- $\beta$  and implications for its removal in Alzheimer's disease. *Drugs & aging*, 21(10), 621-630.
29. Pearson, H. A., & Peers, C. (2006). Physiological roles for amyloid  $\beta$  peptides. *The Journal of physiology*, 575(1), 5-10.
30. Canevari, L., Abramov, A. Y., & Duchon, M. R. (2004). Toxicity of amyloid  $\beta$  peptide: tales of calcium, mitochondria, and oxidative stress. *Neurochemical research*, 29(3), 637-650.
31. Dawson, G. R., Seabrook, G. R., Zheng, H., Smith, D. W., Graham, S., O'dowd, G., ... & Van der Ploeg, L. H. T. (1999). Age-related cognitive deficits, impaired long-term potentiation and reduction in synaptic marker density in mice lacking the  $\beta$ -amyloid precursor protein. *Neuroscience*, 90(1), 1-13.
32. Seabrook, G. R., Smith, D. W., Bowery, B. J., Easter, A., Reynolds, T., Fitzjohn, S. M., ... & Davies, C. H. (1999). Mechanisms contributing to the deficits in hippocampal synaptic plasticity in mice lacking amyloid precursor protein. *Neuropharmacology*, 38(3), 349-359.
33. Kamenetz, F., Tomita, T., Hsieh, H., Seabrook, G., Borchelt, D., Iwatsubo, T., ... & Malinow, R. (2003). APP processing and synaptic function. *Neuron*, 37(6), 925-937.

34. Puzzo, D., Privitera, L., Fa', M., Staniszewski, A., Hashimoto, G., Aziz, F., ... & Jung, S. S. (2011). Endogenous amyloid- $\beta$  is necessary for hippocampal synaptic plasticity and memory. *Annals of neurology*, 69(5), 819-830.
35. Koppensteiner, P., Trinchese, F., Fà, M., Puzzo, D., Gulisano, W., Yan, S., ... & Teich, A. F. (2016). Time-dependent reversal of synaptic plasticity induced by physiological concentrations of oligomeric A $\beta$ 42: an early index of Alzheimer's disease. *Scientific reports*, 6, 32553.
36. Paris, D., Ganey, N., Banasiak, M., Laporte, V., Patel, N., Mullan, M., Murphy, S. F., Yee, G. T., Bachmeier, C., Ganey, C., Beaulieu-Abdelahad, D., Mathura, V. S., Brem, S., & Mullan, M. (2010). Impaired orthotopic glioma growth and vascularization in transgenic mouse models of Alzheimer's disease. *The Journal of neuroscience: the official journal of the Society for Neuroscience*, 30(34), 11251–11258.  
<https://doi.org/10.1523/JNEUROSCI.2586-10.2010>
37. Wei, Y., Zhou, J., Wu, J., & Huang, J. (2019). ER $\beta$  promotes A $\beta$  degradation via the modulation of autophagy. *Cell death & disease*, 10(8), 1-13.
38. Hung, S. Y., Huang, W. P., Liou, H. C., & Fu, W. M. (2015). LC3 overexpression reduces A $\beta$  neurotoxicity through increasing  $\alpha$ 7nAChR expression and autophagic activity in neurons and mice. *Neuropharmacology*, 93, 243-251.
39. Hung, S. Y., Huang, W. P., Liou, H. C., & Fu, W. M. (2009). Autophagy protects neuron from A $\beta$ -induced cytotoxicity. *Autophagy*, 5(4), 502-510
40. Wang, C. S., Wurtman, R. J., & Lee, R. K. (2000). Amyloid precursor protein and membrane phospholipids in primary cortical neurons increase with development, or after exposure to nerve growth factor or A $\beta$ 1–40. *Brain research*, 865(2), 157-167.

41. Plant, L. D., Boyle, J. P., Smith, I. F., Peers, C., & Pearson, H. A. (2003). The production of amyloid  $\beta$  peptide is a critical requirement for the viability of central neurons. *Journal of Neuroscience*, 23(13), 5531-5535
42. Gosztyla, M. L., Brothers, H. M., & Robinson, S. R. (2018). Alzheimer's amyloid- $\beta$  is an antimicrobial peptide: a review of the evidence. *Journal of Alzheimer's Disease*, 62(4), 1495-1506.
43. Soscia, S. J., Kirby, J. E., Washicosky, K. J., Tucker, S. M., Ingelsson, M., Hyman, B., Burton, M. A., Goldstein, L. E., Duong, S., Tanzi, R. E., & Moir, R. D. (2010). The Alzheimer's disease-associated amyloid beta-protein is an antimicrobial peptide. *PloS one*, 5(3), e9505. <https://doi.org/10.1371/journal.pone.0009505>
44. Kumar, D. K. V., Choi, S. H., Washicosky, K. J., Eimer, W. A., Tucker, S., Ghofrani, J., ... & Moir, R. D. (2016). Amyloid- $\beta$  peptide protects against microbial infection in mouse and worm models of Alzheimer's disease. *Science translational medicine*, 8(340), 340ra72-340ra72.
45. Kontush, A., Berndt, C., Weber, W., Akopyan, V., Arlt, S., Schippling, S., & Beisiegel, U. (2001). Amyloid- $\beta$  is an antioxidant for lipoproteins in cerebrospinal fluid and plasma. *Free Radical Biology and Medicine*, 30(1), 119-128.
46. Cull-Candy, S., Brickley, S., & Farrant, M. (2001). NMDA receptor subunits: diversity, development and disease. *Current opinion in neurobiology*, 11(3), 327-335.
47. exidó, L., Martín-Satué, M., Alberdi, E., Solsona, C., & Matute, C. (2011). Amyloid  $\beta$  peptide oligomers directly activate NMDA receptors. *Cell calcium*, 49(3), 184-190. <https://doi.org/10.1016/j.ceca.2011.02.001>

48. Kadir, A., Almkvist, O., Wall, A., Långström, B., & Nordberg, A. (2006). PET imaging of cortical 11 C-nicotine binding correlates with the cognitive function of attention in Alzheimer's disease. *Psychopharmacology*, 188(4), 509-520.
49. Oz, M., Lorke, D. E., Yang, K. H., & Petroianu, G. (2013). On the interaction of  $\beta$ -amyloid peptides and  $\alpha 7$ -nicotinic acetylcholine receptors in Alzheimer's disease. *Current Alzheimer research*, 10(6), 618–630. <https://doi.org/10.2174/15672050113109990132>
50. Wang, H. Y., Li, W., Benedetti, N. J., & Lee, D. H. (2003). Alpha 7 nicotinic acetylcholine receptors mediate beta-amyloid peptide-induced tau protein phosphorylation. *The Journal of biological chemistry*, 278(34), 31547–31553. <https://doi.org/10.1074/jbc.M212532200>
51. Hippus H, Neundörfer G. The discovery of Alzheimer's disease. *Dialogues Clin Neurosci*. 2003;5(1):101-108.
52. Oddo S, Caccamo A, Smith IF, Green KN, LaFerla FM. A dynamic relationship between intracellular and extracellular pools of A $\beta$ . *Am J Pathol*. 2006;168(1):184-194. doi:10.2353/ajpath.2006.050593
53. 2020 Alzheimer's disease facts and figures. (2020). *Alzheimer's & dementia: the journal of the Alzheimer's Association*, 10.1002/alz.12068. Advance online publication. <https://doi.org/10.1002/alz.12068>
54. Whalen, K. (2018). *Lippincott illustrated reviews: pharmacology*. Lippincott Williams & Wilkins.
55. Fisone, G., Borgkvist, A., & Usiello, A. (2004). Caffeine as a psychomotor stimulant: mechanism of action. *Cellular and molecular life sciences : CMLS*, 61(7-8), 857–872. <https://doi.org/10.1007/s00018-003-3269-3>

56. Maia, L., & de Mendonça, A. (2002). Does caffeine intake protect from Alzheimer's disease?. *European journal of neurology*, 9(4), 377–382. <https://doi.org/10.1046/j.1468-1331.2002.00421.x>
57. Cao, C., Cirrito, J. R., Lin, X., Wang, L., Verges, D. K., Dickson, A., ... & Holtzman, D. M. (2009). Caffeine suppresses amyloid- $\beta$  levels in plasma and brain of Alzheimer's disease transgenic mice. *Journal of Alzheimer's Disease*, 17(3), 681-697.
58. Ritchie, K., Carrière, I., De Mendonça, A., Portet, F., Dartigues, J. F., Rouaud, O., ... & Ancelin, M. L. (2007). The neuroprotective effects of caffeine: a prospective population study (the Three City Study). *Neurology*, 69(6), 536-545.
59. Van Gelder, B. M., Buijsse, B., Tijhuis, M., Kalmijn, S., Giampaoli, S., Nissinen, A., & Kromhout, D. (2007). Coffee consumption is inversely associated with cognitive decline in elderly European men: the FINE Study. *European journal of clinical nutrition*, 61(2), 226-232.
60. Wongprayoon, P., & Govitrapong, P. (2015). Melatonin attenuates methamphetamine-induced neuroinflammation through the melatonin receptor in the SH-SY5Y cell line. *Neurotoxicology*, 50, 122-130.
61. Zhao, J., Sun, X., Yu, Z., Pan, X., Gu, F., Chen, J., ... & Zhong, C. (2011). Exposure to pyriithiamine increases  $\beta$ -amyloid accumulation, Tau hyperphosphorylation, and glycogen synthase kinase-3 activity in the brain. *Neurotoxicity research*, 19(4), 575-583.
62. Chen, L., Zhou, L., Yu, P., Fang, F., Jiang, L., Fei, J., ... & Wang, J. (2019). Methamphetamine exposure upregulates the amyloid precursor protein and hyperphosphorylated tau expression: The roles of insulin signaling in SH-SY5Y cell line. *The Journal of toxicological sciences*, 44(7), 493-503.

63. Demuro, A., Mina, E., Kaye, R., Milton, S. C., Parker, I., & Glabe, C. G. (2005). Calcium dysregulation and membrane disruption as a ubiquitous neurotoxic mechanism of soluble amyloid oligomers. *Journal of Biological Chemistry*, 280(17), 17294-17300.
64. Kam, T. I., Gwon, Y., & Jung, Y. K. (2014). Amyloid beta receptors responsible for neurotoxicity and cellular defects in Alzheimer's disease. *Cellular and molecular life sciences*, 71(24), 4803-4813.
65. Ron, D., & Walter, P. (2007). Signal integration in the endoplasmic reticulum unfolded protein response. *Nature reviews Molecular cell biology*, 8(7), 519-529
66. McCullough, K. D., Martindale, J. L., Klotz, L. O., Aw, T. Y., & Holbrook, N. J. (2001). Gadd153 sensitizes cells to endoplasmic reticulum stress by down-regulating Bcl2 and perturbing the cellular redox state. *Molecular and cellular biology*, 21(4), 1249-1259.
67. Huang, X., Chen, Y., Zhang, H., Ma, Q., Zhang, Y. W., & Xu, H. (2012). Salubrinal attenuates  $\beta$ -amyloid-induced neuronal death and microglial activation by inhibition of the NF- $\kappa$ B pathway. *Neurobiology of aging*, 33(5), 1007-e9
68. Michalak, M., Parker, J. R., & Opas, M. (2002).  $Ca^{2+}$  signaling and calcium binding chaperones of the endoplasmic reticulum. *Cell calcium*, 32(5-6), 269-278.
69. Kam, T. I., Gwon, Y., & Jung, Y. K. (2014). Amyloid beta receptors responsible for neurotoxicity and cellular defects in Alzheimer's disease. *Cellular and molecular life sciences*, 71(24), 4803-4813.
70. Chen, Guo-fang, et al. "Amyloid beta: structure, biology and structure-based therapeutic development." *Acta Pharmacologica Sinica* 38.9 (2017): 1205-1235.

71. Lustbader, J. W., Cirilli, M., Lin, C., Xu, H. W., Takuma, K., Wang, N., ... & Trinchese, F. (2004). ABAD directly links A $\beta$  to mitochondrial toxicity in Alzheimer's disease. *Science*, 304(5669), 448-452
72. Du, H., Guo, L., Fang, F., Chen, D., Sosunov, A. A., McKhann, G. M., ... & Gunn-Moore, F. J. (2008). Cyclophilin D deficiency attenuates mitochondrial and neuronal perturbation and ameliorates learning and memory in Alzheimer's disease. *Nature medicine*, 14(10), 1097-1105.
73. Henderson, G. L. (1988). Designer drugs: past history and future prospects. *Journal of Forensic Science*, 33(2), 569-575
74. Liechti, M. E. (2015). Novel psychoactive substances (designer drugs): overview and pharmacology of modulators of monoamine signalling. *Swiss medical weekly*, 145, w14043
75. Gee, P., Richardson, S., Woltersdorf, W., & Moore, G. (2005). Toxic effects of BZP-based herbal party pills in humans: a prospective study in Christchurch, New Zealand. *The New Zealand Medical Journal (Online)*, 118(1227).
76. Arbo, M. D., Bastos, M. L., & Carmo, H. F. (2012). Piperazine compounds as drugs of abuse. *Drug and alcohol dependence*, 122(3), 174-185.
77. Haroz, R., & Greenberg, M. I. (2006). New drugs of abuse in North America. *Clinics in laboratory medicine*, 26(1), 147-164.
78. Wikström, M., Holmgren, P., & Ahlner, J. (2004). A2 (N-benzylpiperazine) a new drug of abuse in Sweden. *Journal of analytical toxicology*, 28(1), 67-70.
79. Drug Enforcement Administration (DEA), Department of Justice. (2004). Schedules of controlled substances; placement of 2, 5-dimethoxy-4-(n)-propylthiophenethylamine and



N-benzylpiperazine into Schedule I of the Controlled Substances Act. Final rule. Federal register, 69(53), 12794

80. Baumann, M. H., Clark, R. D., Budzynski, A. G., Partilla, J. S., Blough, B. E., & Rothman, R. B. (2005). N-substituted piperazines abused by humans mimic the molecular mechanism of 3, 4-methylenedioxymethamphetamine (MDMA, or 'Ecstasy'). *Neuropsychopharmacology*, 30(3), 550-560
81. Dhanasekaran, M. (2018). Global Health Impact of Major Classes of "Designer Drugs": Structural, Pharmacological and Toxicological Overview.
82. Wells, B. G., DiPiro, J. T., Schwinghammer, T. L., & DiPiro, C. V. (2014). *Pharmacotherapy Handbook*, 9/E. McGraw Hill Professional.
83. Hippus, H., & Neundörfer, G. (2003). The discovery of Alzheimer's disease. *Dialogues in clinical neuroscience*, 5(1), 101.
84. Bekris, L. M., Yu, C. E., Bird, T. D., & Tsuang, D. W. (2010). Genetics of Alzheimer disease. *Journal of geriatric psychiatry and neurology*, 23(4), 213–227. <https://doi.org/10.1177/0891988710383571>
85. Dorszewska, J., Prendecki, M., Oczkowska, A., Dezor, M., & Kozubski, W. (2016). Molecular basis of familial and sporadic Alzheimer's disease. *Current Alzheimer Research*, 13(9), 952-96
86. Edwards Iii, G. A., Gamez, N., Escobedo, G., Jr, Calderon, O., & Moreno-Gonzalez, I. (2019). Modifiable Risk Factors for Alzheimer's Disease. *Frontiers in aging neuroscience*, 11, 146. <https://doi.org/10.3389/fnagi.2019.00146>

87. Bayer, T. A., & Wirths, O. (2010). Intracellular accumulation of amyloid-Beta-a predictor for synaptic dysfunction and neuron loss in Alzheimer's disease. *Frontiers in aging neuroscience*, 2,8.
88. Prince, M., Comas-Herrera, A., Knapp, M., Guerchet, M., & Karagiannidou, M. (2016). World Alzheimer report 2016: improving healthcare for people living with dementia: coverage, quality and costs now and in the future.
89. Hebert, L. E., Weuve, J., Scherr, P. A., & Evans, D. A. (2013). Alzheimer disease in the United States (2010–2050) estimated using the 2010 census. *Neurology*, 80(19), 1778-1783.
90. Alzheimer's Association. (2012). 2012 Alzheimer's disease facts and figures. *Alzheimer's & Dementia*, 8(2), 131-168
91. Sondag, C. M., Dhawan, G., & Combs, C. K. (2009). Beta amyloid oligomers and fibrils stimulate differential activation of primary microglia. *Journal of neuroinflammation*, 6, 1. <https://doi.org/10.1186/1742-2094-6-1>
92. White, J. A., Manelli, A. M., Holmberg, K. H., Van Eldik, L. J., & Ladu, M. J. (2005). Differential effects of oligomeric and fibrillar amyloid-beta 1-42 on astrocyte-mediated inflammation. *Neurobiology of disease*, 18(3), 459–465. <https://doi.org/10.1016/j.nbd.2004.12.013>
93. Kinney, J. W., Bemiller, S. M., Murtishaw, A. S., Leisgang, A. M., Salazar, A. M., & Lamb, B. T. (2018). Inflammation as a central mechanism in Alzheimer's disease. *Alzheimer's & dementia (New York, N. Y.)*, 4, 575–590. <https://doi.org/10.1016/j.trci.2018.06.014>

94. Sarma, J. D. (2014). Microglia-mediated neuroinflammation is an amplifier of virus-induced neuropathology. *Journal of neurovirology*, 20(2), 122-136.
95. Glenn, J. A., Jordan, F. L., & Thomas, W. E. (1989). Further studies on the identification of microglia in mixed brain cell cultures. *Brain research bulletin*, 22(6), 1049-1052.
96. Bolmont, T., Haiss, F., Eicke, D., Radde, R., Mathis, C. A., Klunk, W. E., ... & Calhoun, M. E. (2008). Dynamics of the microglial/amyloid interaction indicate a role in plaque maintenance. *Journal of Neuroscience*, 28(16), 4283-4292.
97. Hickman, S. E., Allison, E. K., & El Khoury, J. (2008). Microglial dysfunction and defective  $\beta$ -amyloid clearance pathways in aging Alzheimer's disease mice. *Journal of Neuroscience*, 28(33), 8354-8360.
98. Meda, L., Cassatella, M. A., Szendrei, G. I., Otvos, L., Baron, P., Villalba, M., ... & Rossi, F. (1995). Activation of microglial cells by  $\beta$ -amyloid protein and interferon- $\gamma$ . *Nature*, 374(6523), 647-650.
99. Akiyama, H., Barger, S., Barnum, S., Bradt, B., Bauer, J., Cole, G. M., ... & Finch, C. E. (2000). Inflammation and Alzheimer's disease. *Neurobiology of aging*, 21(3), 383-421
- Hang, R., Yee, K. L., & Sumbria, R. K. (2017). Tumor necrosis factor  $\alpha$  Inhibition for Alzheimer's Disease. *Journal of central nervous system disease*, 9, 117957351770927
100. Combs, C. K., Karlo, J. C., Kao, S. C., & Landreth, G. E. (2001).  $\beta$ -Amyloid stimulation of microglia and monocytes results in TNF $\alpha$ -dependent expression of inducible nitric oxide synthase and neuronal apoptosis. *Journal of Neuroscience*, 21(4), 1179-1188.
101. Yamamoto, K., Arakawa, T., Ueda, N., & Yamamoto, S. (1995). Transcriptional roles of nuclear factor B and nuclear factor-interleukin-6 in the tumor necrosis factor-

- dependent induction of cyclooxygenase-2 in MC3T3-E1 cells. *Journal of Biological Chemistry*, 270(52), 31315-31320.
102. Mitra S, Prasad P, Chakraborty S. A Unified View of Assessing the Pro-oxidant versus Antioxidant Nature of Amyloid Beta Conformers. *Chembiochem*. 2018;19(22):2360-2371. doi:10.1002/cbic.201800446
103. Yan, S. D., & Stern, D. M. (2005). Mitochondrial dysfunction and Alzheimer's disease: role of amyloid- $\beta$  peptide alcohol dehydrogenase (ABAD). *International journal of experimental pathology*, 86(3), 161-171.
104. Fredholm, B. B., Bättig, K., Holmén, J., Nehlig, A., & Zvartau, E. E. (1999). Actions of caffeine in the brain with special reference to factors that contribute to its widespread use. *Pharmacological reviews*, 51(1), 83-133
105. Arendash, G. W., Schleif, W., Rezai-Zadeh, K., Jackson, E. K., Zacharia, L. C., Cracchiolo, J. R., ... & Tan, J. (2006). Caffeine protects Alzheimer's mice against cognitive impairment and reduces brain  $\beta$ -amyloid production. *Neuroscience*, 142(4), 941-952.
106. de Angelis, C., Nardone, A., Garifalos, F., Pivonello, C., Sansone, A., Conforti, A., ... & Colao, A. (2020). Smoke, alcohol and drug addiction and female fertility. *Reproductive Biology and Endocrinology*, 18(1), 1-26.
107. Ciani, F., Cocchia, N., d'Angelo, D., & Tafuri, S. (2015). Influence of ROS on ovarian functions. *New Discov Embryol*, 3, 1-34.
108. Ramesh, S., Govindarajulu, M., Lynd, T., Briggs, G., Adamek, D., Jones, E., ... & Suppiramaniam, V. (2018). SIRT3 activator Honokiol attenuates  $\beta$ -Amyloid by modulating amyloidogenic pathway. *PLoS One*, 13(1), e0190350.

109. Ahuja, M., Buabeid, M., Abdel-Rahman, E., Majrashi, M., Parameshwaran, K., Amin, R., ... & Dhanasekaran, M. (2017). Immunological alteration & toxic molecular inductions leading to cognitive impairment & neurotoxicity in transgenic mouse model of Alzheimer's disease. *Life Sciences*, 177, 49-59.
110. Wills, E. D. (1965). Mechanisms of lipid peroxide formation in tissues role of metals and haematin proteins in the catalysis of the oxidation of unsaturated fatty acids. *Biochimica et Biophysica Acta (BBA)-Lipids and Lipid Metabolism*, 98(2), 238-251
111. Ramsay, R. R., Salach, J. I., Dadgar, J., & Singer, T. P. (1986). Inhibition of mitochondrial NADH dehydrogenase by pyridine derivatives and its possible relation to experimental and idiopathic parkinsonism. *Biochemical and biophysical research communications*, 135(1), 269–275. [https://doi.org/10.1016/0006-291x\(86\)90972-1](https://doi.org/10.1016/0006-291x(86)90972-1)
112. Zheng, M., Ahuja, M., Bhattacharya, D., Clement, T. P., Hayworth, J. S., & Dhanasekaran, M. (2014). Evaluation of differential cytotoxic effects of the oil spill dispersant Corexit 9500. *Life sciences*, 95(2), 108-117
113. Usha, R., Muralikrishnan, D., Thomas, B., Ghosh, S., Mandal, C., & Mohanakumar, K. P. (2000). Region-specific attenuation of a trypsin-like protease in substantia nigra following dopaminergic neurotoxicity by 1-methyl-4-phenyl-1, 2, 3, 6-tetrahydropyridine. *Brain research*, 882(1-2), 191-195.
114. Copeland, R. A., Williams, J. M., Giannaras, J., Nurnberg, S., Covington, M., Pinto, D., ... & Trzaskos, J. M. (1994). Mechanism of selective inhibition of the inducible isoform of prostaglandin G/H synthase. *Proceedings of the National Academy of Sciences*, 91(23), 11202-11206.

115. Thapa, A., & Carroll, N. J. (2017). Dietary modulation of oxidative stress in Alzheimer's disease. *International journal of molecular sciences*, 18(7), 158
116. Hardy, J., & Selkoe, D. J. (2002). The amyloid hypothesis of Alzheimer's disease: progress and problems on the road to therapeutics. *Science (New York, N.Y.)*, 297(5580), 353–356. <https://doi.org/10.1126/science.1072994>
117. Kozłowski, H., Luczkowski, M., Remelli, M., & Valensin, D. (2012). Copper, zinc and iron in neurodegenerative diseases (Alzheimer's, Parkinson's and prion diseases). *Coordination Chemistry Reviews*, 256(19-20), 2129-2141.
118. Cheignon, C., Tomas, M., Bonnefont-Rousselot, D., Faller, P., Hureau, C., & Collin, F. (2018). Oxidative stress and the amyloid beta peptide in Alzheimer's disease. *Redox biology*, 14, 450-464.
119. Nunomura, A., Perry, G., Aliev, G., Hirai, K., Takeda, A., Balraj, E. K., Jones, P. K., Ghanbari, H., Wataya, T., Shimohama, S., Chiba, S., Atwood, C. S., Petersen, R. B., & Smith, M. A. (2001). Oxidative damage is the earliest event in Alzheimer disease. *Journal of neuropathology and experimental neurology*, 60(8), 759–767. <https://doi.org/10.1093/jnen/60.8.759>
121. Anekonda, T. S., & Reddy, P. H. (2005). Can herbs provide a new generation of drugs for treating Alzheimer's disease?. *Brain research. Brain research reviews*, 50(2), 361–376. <https://doi.org/10.1016/j.brainresrev.2005.09.001>
122. Gemma, C., Vila, J., Bachstetter, A., & Bickford, P. C. (2007). Oxidative Stress and the Aging Brain: From Theory to Prevention. In D. R. Riddle (Ed.), *Brain Aging: Models, Methods, and Mechanisms*. CRC Press/Taylor & Francis.

123. Ferreira, L.G.; dos Santos, R.N.; (2015) Molecular docking and structure-based drug design strategies. *Molecules*. 20. 13384-13421
124. Hroudová, J., Singh, N., & Fišar, Z. (2014). Mitochondrial dysfunctions in neurodegenerative diseases: relevance to Alzheimer's disease. *BioMed research international*, 2014
125. Roth, K. A. (2001). Caspases, apoptosis, and Alzheimer disease: causation, correlation, and confusion. *Journal of Neuropathology & Experimental Neurology*, 60(9), 829-838
126. Nicholson, D. W. (2000). From bench to clinic with apoptosis-based therapeutic agents. *Nature*, 407(6805), 810-816.
127. Li, S., Geiger, N. H., Soliman, M. L., Hui, L., Geiger, J. D., & Chen, X. (2015). Caffeine, Through Adenosine A3 Receptor-Mediated Actions, Suppresses Amyloid- $\beta$  Protein Precursor Internalization and Amyloid- $\beta$  Generation. *Journal of Alzheimer's disease: JAD*, 47(1), 73–83. <https://doi.org/10.3233/JAD-142223>.